# A GPS and modelling study of deformation in northern Central America

M. Rodriguez,[1] C. DeMets,[1] R. Rogers,[2] C. Tenorio[3] and D. Hernandez[4]

[1]*Geology and Geophysics, University of Wisconsin-Madison, Madison, WI 53706 USA. E-mail: chuck@geology.wisc.edu*
[2]*Department of Geology, California State University Stanislaus, Turlock, CA 95382, USA*
[3]*School of Physics, Faculty of Sciences, Universidad Nacional Autonoma de Honduras, Tegucigalpa, Honduras*
[4]*Servicio Nacional de Estudios Territoriales, Ministerio de Medio Ambiente y Recursos Naturales, Km. 5 1/2 carretera a Santa Tecla, Colonia y Calle Las Mercedes, Plantel ISTA, San Salvador, El Salvador*

## SUMMARY

We use GPS measurements at 37 stations in Honduras and El Salvador to describe active deformation of the western end of the Caribbean Plate between the Motagua fault and Central American volcanic arc. All GPS sites located in eastern Honduras move with the Caribbean Plate, in accord with geologic evidence for an absence of neotectonic deformation in this region. Relative to the Caribbean Plate, the other stations in the study area move west to west–northwest at rates that increase gradually from $3.3 \pm 0.6$ mm yr$^{-1}$ in central Honduras to $4.1 \pm 0.6$ mm yr$^{-1}$ in western Honduras to as high as 11–12 mm yr$^{-1}$ in southern Guatemala. The site motions are consistent with slow westward extension that has been inferred by previous authors from the north-striking grabens and earthquake focal mechanisms in this region. We examine the factors that influence the regional deformation by comparing the new GPS velocity field to velocity fields predicted by finite element models (FEMs) that incorporate the regional plate boundary faults and known plate motions. Our modelling suggests that the obliquely convergent ($\sim 20°$) direction of Caribbean–North American Plate motion relative to the Motagua fault west of 90°W impedes the ENE-directed motion of the Caribbean Plate in southern Guatemala, giving rise to extension in southern Guatemala and western Honduras. The FEM predictions agree even better with the measured velocities if the plate motion west of the Central American volcanic arc is forced to occur over a broad zone rather than along a single throughgoing plate boundary fault. Our analysis confirms key predictions of a previous numerical model for deformation in this region, and also indicates that the curvature of the Motagua fault causes significant along-strike changes in the orientations of the principal strain-rate axes in the fault borderlands, in accord with earthquake focal mechanisms and conclusions reached in a recent synthesis of the structural and morphologic data from Honduras. Poor fits of our preferred models to the velocities of GPS sites near the Gulf of Fonseca may be an artefact of the still-short GPS time-series in this region or the simplifying assumptions of our FEMs.

**Key words:** Space geodetic surveys; Continental tectonics: extensional; Dynamics: seismotectonics; Neotectonics.

GJI Tectonics and geodynamics

## 1 INTRODUCTION

The 3500-km-long boundary between the Caribbean and North American Plates extends through northern Central America along its westernmost 500 km (Fig. 1), where plate motion is accommodated by deformation across a wide zone that includes the Motagua and Polochic strike-slip faults of Guatemala, grabens in Honduras and southern Guatemala (Plafker 1976; Burkart & Self 1985; Manton 1987; Rogers & Mann 2007), and strike-slip and reverse faults in southern Mexico (Guzman-Speziale & Meneses-Rocha

2000). Numerous authors have speculated about the factors that give rise to the complex and wide plate boundary. Malfait & Dinkelman (1972) and Burkart (1983) hypothesize that extension across the grabens south of the Motagua and Polochic faults occurs in response to a combination of slow eastward motion of the Caribbean Plate and pinning of the western, wedge-shaped end of the Caribbean Plate between the Middle America trench and the westward-moving North American Plate (Fig. 2). Burkart & Self (1985) further suggest that the lithosphere located south of the arcuate, convex-to-the-south Motagua fault is forced to extend as it moves along the
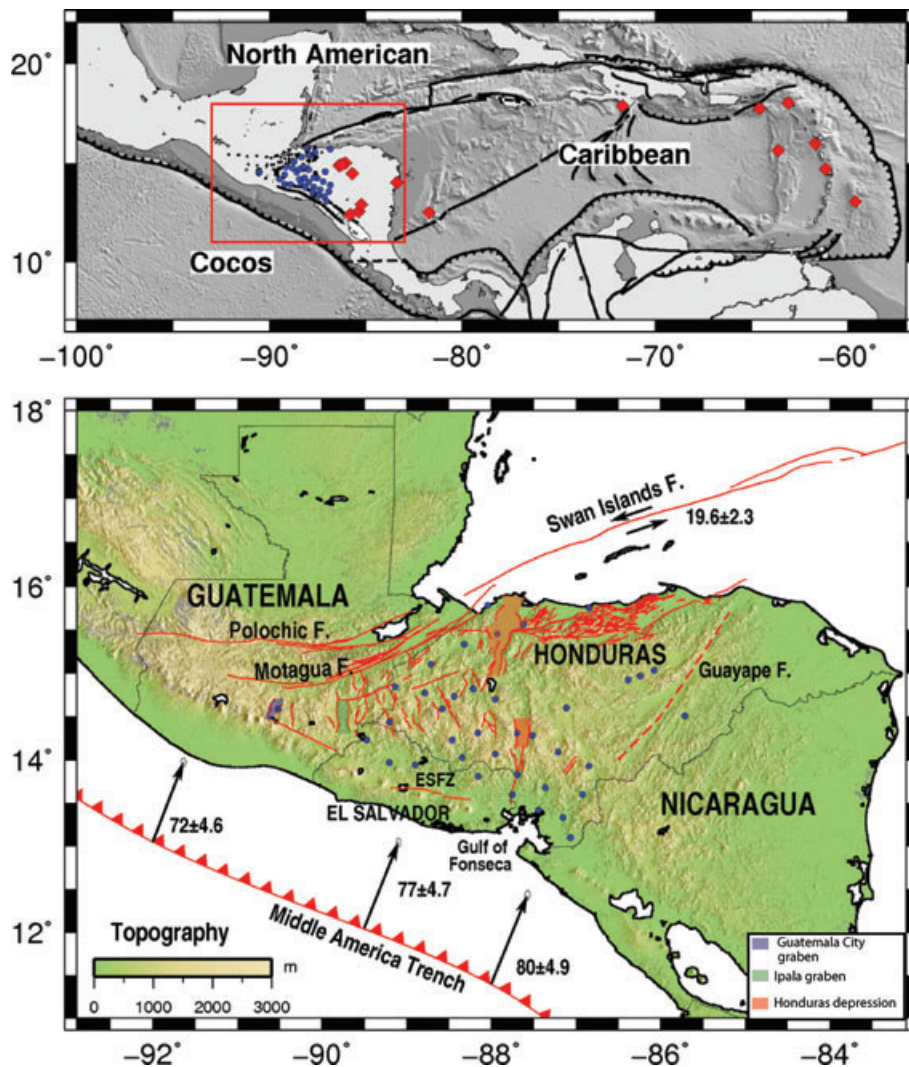
**Figure 1.** Upper panel: plate tectonic setting of the study area. Blue symbols show locations of GPS sites whose motions are used to study deformation inland from the Central American volcanic arc. Red diamonds show locations of GPS stations whose motions are used to determine the angular velocity of the Caribbean Plate relative to ITRF2005. Rectangle indicates limits of the study area. Lower panel: active faults (red lines) and geography of northern Central America. Blue circles indicate locations of GPS stations used in this study. Arrows indicate relative plate velocities in mm yr$^{-1}$ and are from DeMets (2001) for the Cocos–Caribbean Plate boundary and from this study for the Caribbean–North America boundary. Topography is from 90-m Shuttle Topography Radar Mission (STRM) data from *seamless.usgs.gov.* Fault locations in Honduras and southern Guatemala are from Rogers (2003). 'ESFZ' is El Salvador Fault Zone from Corti *et al.* (2005).

curved fault trace in response to the plate motion. Guzman-Speziale *et al.* (1989) and Guzman-Speziale & Meneses-Rocha (2000) postulate that distributed deformation in southern Mexico, north of the Motagua–Polochic fault zone, may occur in response to difficulties in transferring the plate motion across the Chiapas Massif of southern Mexico and suggest that the plate motion dies out before it reaches the Middle America trench.

In order to better understand the factors that control deformation across this wide plate boundary, Alvarez-Gomez *et al.* (2008) attempt to match the regional pattern of stresses derived from seismic moment tensors with finite element models (FEMs) that simulate the geometries of the major faults in northern Central America and are driven by the regional plate motions. From FEMs that impose a series of boundary and fault-slip constraints appropriate for the region, they find that the most successful models have four primary characteristics. First, the forces that resist subduction of the Cocos Plate must be weak in comparison to the forces that drive

the eastward motion of the Caribbean Plate (Fig. 2). Second, the Central American volcanic arc must be rheologically weak. Third, the Guatemalan forearc must be pinned to the North American Plate, thereby precluding a narrow boundary between the Caribbean and North America Plates between the western terminus of the Polochic fault and trench. Finally, the orientation of the strike-slip plate boundary faults relative to the direction of Caribbean–North America motion is important for capturing the regional deformation. Important elements of the conceptual framework outlined by earlier authors (Fig. 2) are thus supported by this modelling study.

Seismic and geodetic measurements of active deformation in northern Central America have lagged behind other regions due to the slow deformation rates and logistical factors. The first quantitative measures of active deformation across the broad extending zone in Honduras and Guatemala south of the plate boundary were determined from the moment tensors of scattered, small earthquakes
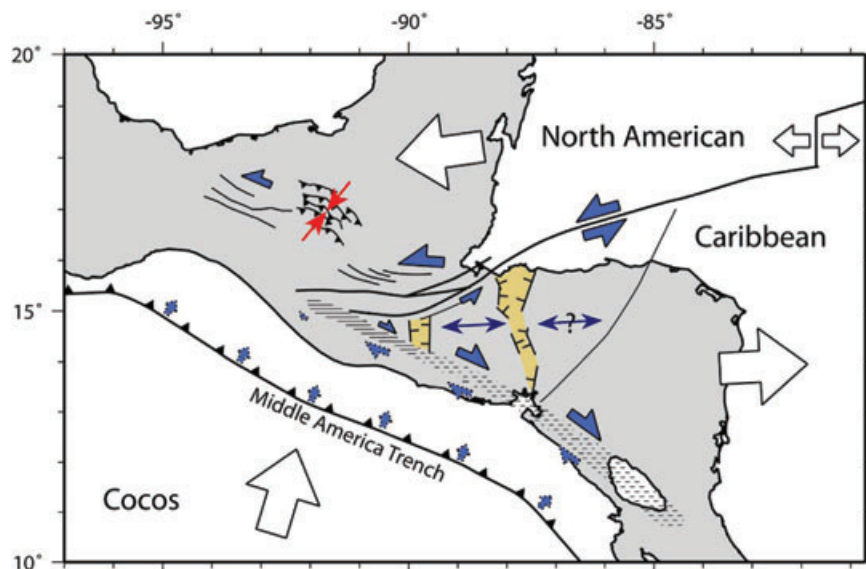
**Figure 2.** Conceptual model for forces that may determine the present deformation in northern Central America, adapted from Alvarez-Gomez *et al.* (2008). Colored arrows approximate relative motions across the major faults in the study area and open arrows approximate the directions of motion of the major plates relative to a fixed mantle reference frame. Arrows are not drawn to scale.

in the Guatemalan and Honduran grabens (Guzman-Speziale 2001; Caceres *et al.* 2005). Both studies indicate that deformation is dominated by slow, E–W to WNW–ESE stretching. Due to the short record of seismicity, the seismic stretching rate is only loosely constrained, with limits of 1–15 mm yr$^{-1}$ (8 ± 7 mm yr$^{-1}$).

The first geodetic measurements pertinent to the Caribbean–North America Plate boundary in this region were reported by Lyon-Caen *et al.* (2006), who document evidence for 20 mm yr$^{-1}$ of boundary-parallel slip along the Motagua and Polochic faults of Guatemala and 11–12 mm yr$^{-1}$ of east–west stretching between sites in southern Guatemala and the Caribbean Plate interior. The latter estimate corroborates the seismically derived direction and stretching rate documented by Guzman-Speziale (2001) and Caceres *et al.* (2005) and shows for the first time that more than half of the strike-slip motion that occurs along the Motagua and Polochic faults in easternmost Guatemala is ultimately transferred southwards into the grabens of Honduras and Guatemala.

Herein, we report velocities for a GPS network that spans nearly all of the broad extending zone in Honduras and Guatemala (Fig. 1). The new network includes 33 GPS stations in Honduras, many more than the single Honduran station velocity that was employed by previous authors (Lyon-Caen *et al.* 2006; DeMets *et al.* 2007) to document motion within deforming areas of Honduras. The new GPS velocity field confirms previously described evidence for pervasive stretching south of the Motagua fault, but reveals previously unknown details of the east to west deformation-rate gradient and subtle changes in the directions of deformation. We use finite element modelling to examine the possible causes of the observed deformation, including whether deformation is influenced significantly by the changing orientation of the Motagua fault in Central America relative to the direction of plate motion, whether the wedge-shaped geometry of the western end of the Caribbean Plate influences the pattern of deformation, and whether the assumed width of the poorly understood plate boundary zone west of the Central American volcanic arc affects the regional deformation pattern.

## 2 TECTONIC SETTING OF THE STUDY AREA

Northern Central America, which includes the countries of El Salvador, Guatemala, Honduras, and parts of Nicaragua and southern Mexico, is a tectonically defined, wedge-shaped region at the western end of the Caribbean Plate bordered by the Middle America trench and Motagua–Polochic fault zone (Fig. 1). The primary tectonic features in the region are the Middle America subduction zone (Fig. 3), which accommodates 70–80 mm yr$^{-1}$ of northeastward Cocos–Caribbean Plate subduction (Fig. 1), and strike-slip faults in Central America and the Caribbean Sea that accommodate 19–20 mm yr$^{-1}$ of left-lateral, strike-slip motion between the Caribbean and North American Plates. The submarine Swan Islands fault carries the plate motion west from the Cayman spreading centre to eastern Guatemala (Rosencrantz & Mann 1991), where motion is transferred to the Motagua and Polochic faults of Guatemala. The Jocotan-Chamelecon fault system in Guatemala and Honduras may also accommodate some motion, although no geological or other evidence for Holocene age slip has been reported for either of these faults (Schwartz *et al.* 1979; Ferrari *et al.* 1994; Gordon & Muehlberger 1994).

### 2.1 Motagua and Polochic faults

Field and aerial studies of the Motagua and Polochic faults have established their total offsets and demonstrate that the two faults have accommodated most Caribbean–North America Plate motion over the past 5–10 Myr (Muehlberger & Ritchie 1975; Plafker 1976; Burkart 1978; Schwartz *et al.* 1979; Burkart 1983; Burkart *et al.* 1987). The 1976 February 4, $M_s$ = 7.5 Motagua fault earthquake, which killed more than 20 000 people and left homeless nearly 20 per cent of the population of Guatemala (Plafker 1976), clearly established the Motagua fault's role as an active part of the plate boundary. Similarly, the 1816 July 22, $M_w$ ∼ 7.5 earthquake on the Polochic fault established that this fault is also an important,
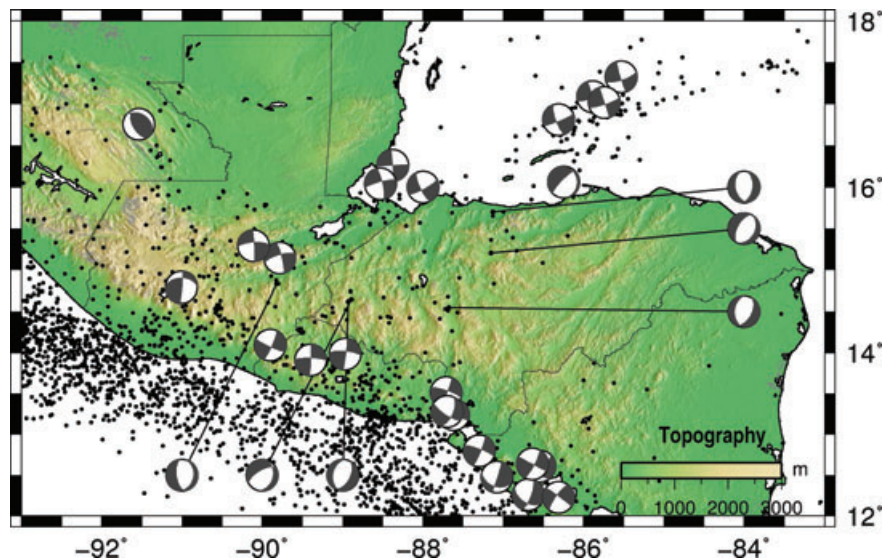
**Figure 3.** Seismicity in northern Central America. Earthquakes above depths of 50 km and with $M_w \geq 3$ for the period 1973–2008 from the National Earthquake Information Center data base are shown. Focal mechanisms are Harvard centroid-moment tensor solutions for the period 1976–2008.

seismically hazardous part of the present plate boundary (White 1985).

Lyon-Caen *et al.* (2006) report recent slip rates for these two faults from GPS measurements at sites in eastern and central Guatemala. Elastic modelling of the motions measured at seven GPS sites that span the two faults in eastern Guatemala indicates that the GPS motions are well fit for models in which the summed slip rate for the two faults is 20 mm yr$^{-1}$, of which 0–5 mm yr$^{-1}$ of slip occurs on the Polochic fault and the remainder on the Motagua fault. The estimated slip rate is equal to the Caribbean–North America rate predicted from sites located in the interiors of these two plates (DeMets *et al.* 2007), thereby indicating that most or all of the boundary-parallel component of the plate motion is accommodated in a narrow zone where the slip comes onshore in eastern Guatemala.

Farther west in central Guatemala, the motions of five GPS stations that span the two faults are best fit by an elastic model in which their combined slip rate is only 12 mm yr$^{-1}$ (Lyon-Caen *et al.* 2006). The difference in the slip rate estimates for eastern and central Guatemala indicates that $\approx$8 mm yr$^{-1}$ of plate motion is transferred to structures in the borderlands of the Motagua and Polochic faults between eastern and central Guatemala.

## 2.2 Extension in Honduras and southern Guatemala

The 1976 February 4 Motagua fault earthquake triggered numerous smaller earthquakes along normal faults south of the Motagua fault (Matumoto & Latham 1976; Langer & Bollinger 1979), highlighting the tectonic relationship between the prominent strike-slip faults of Guatemala and the grabens of Honduras and southern Guatemala (Plafker 1976; Manton 1987; Rogers & Mann 2007). Early studies of the structures and geomorphology of southern Guatemala and central Honduras concluded that both regions extend actively (Plafker 1976; Manton 1987), in accord with seismic evidence for recent and historic earthquakes in this region (Langer & Bollinger 1979; Osiecki 1981). GPS measurements from two sites in southern Guatemala and one site in central Honduras (Lyon-Caen *et al.* 2006) indicate that 11–12 mm yr$^{-1}$ of east–west stretching occurs across the extending zone in Honduras and Guatemala. Consequently, 60 per cent or possibly more of the plate motion along the Motagua

and Polochic faults in eastern Guatemala is ultimately transferred southwards into the grabens of Honduras and Guatemala.

Recent syntheses of geological and geophysical data from Honduras and offshore areas (Rogers *et al.* 2002; Rogers & Mann 2007) divide the country into four morphotectonic zones (shown in Fig. 4). The largest and most tectonically active zone is in western Honduras (zone 1), where active rifting occurs. The rifts in this zone are generally well defined, are often half-grabens, and trend locally orthogonal to the Motagua and Polochic faults in the western reaches of this zone and northwards in the eastern reaches of this zone. A second tectonically active province parallels the north coast of Honduras (zone 4) and extends offshore to the Swan Islands fault. Deformation in this zone is characterized by NNW–SSE extension across faults that are subparallel to the Swan Islands fault. A study of uplifted coastal landforms off the north coast of Honduras, within zone 4, indicates that large magnitude earthquakes ($M > 7$) recur in this region every $\sim$1000 yr (Cox *et al.* 2008) and pose substantial seismic and tsunami hazards to the coastal and near-coastal land areas in this region.

Rogers *et al.* (2002) and Rogers & Mann (2007) also describe two tectonically inactive regions in Honduras (zones 2 and 3). Zone 2 is subdivided into a 700-m to 1000-m-high plateau in the interior of Honduras that consists of an undeformed, aseismic core plateau (zone 2b) and a region of apparently inactive rifts (zone 2a) where some earthquakes occur (Fig. 3). Rogers *et al.* (2002) define zone 3 as the undeformed, seismically inactive part of Honduras east of the Guayape fault. Rogers *et al.* (2002) also note an absence of morphologic and seismic evidence for recent slip along the prominent Guayape fault between zones 2 and 3. Measurements at four GPS stations in zones 2b and 3 spanning the Guayupe fault suggest an upper bound of $\approx$2 mm yr$^{-1}$ for any slip along this fault (DeMets *et al.* 2007), in accord with the geomorphologic evidence for its apparent inactivity, however contrary to arguments presented by Gordon & Muehlberger (1994) for active dextral strike-slip motion along this fault.

## 2.3 Distributed deformation in southern Mexico

Structural and seismic data also suggest that some motion along the Motagua and possibly Polochic faults in eastern Guatemala is
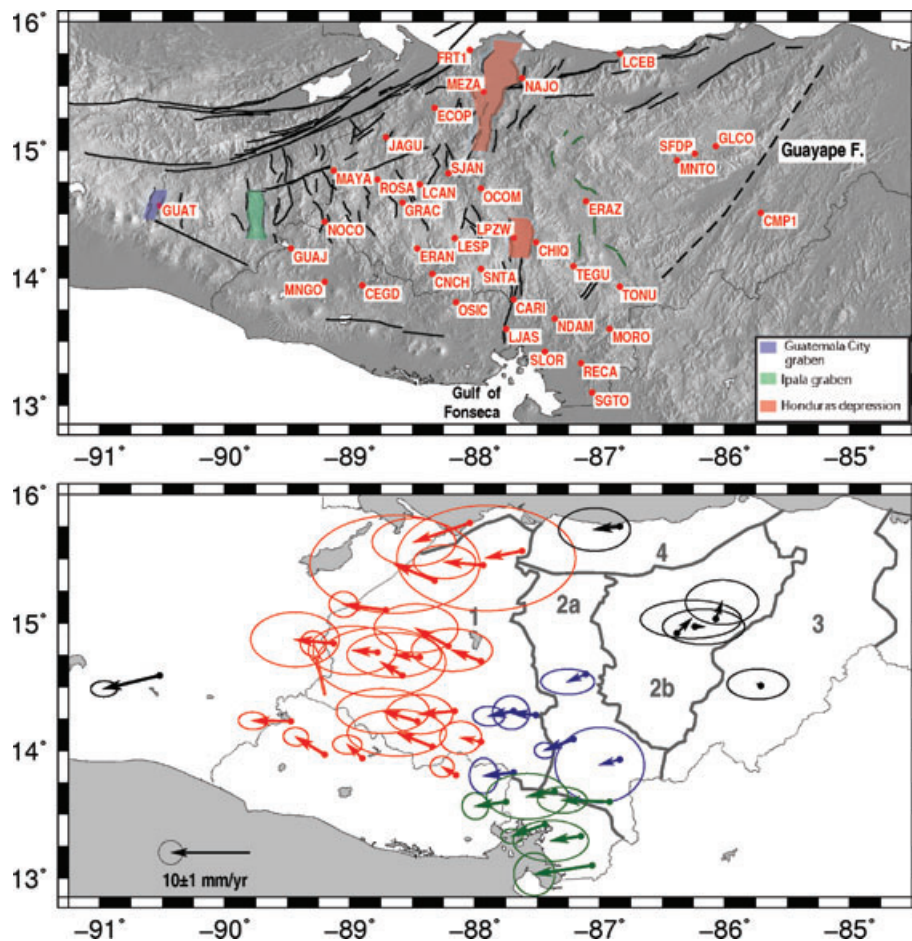
**Figure 4.** Upper panel: locations and names of GPS sites employed for the analysis and grabens discussed in the text. Faults shown with black lines are active and with green lines, inactive (Rogers 2003). Lower panel: GPS station velocities in Caribbean Plate reference frame with 2-D, 1-σ uncertainties. Grey lines identify morphotectonic provinces in Honduras defined by Rogers *et al.* (2002) and Rogers & Mann (2007), as follows: zone 1 – Active rifts; zone 2a – Inactive rifts; 2b – Honduran plateau; zone 3 – Eastern province; zone 4 – North coast province. Colours of the velocity arrows represent different velocity field patterns discussed in the text.

transferred northward to faults in southern Mexico. Guzman-Speziale *et al.* (1989) and Guzman-Speziale & Meneses-Rocha (2000) describe evidence for active faulting along northwest-trending strike-slip and thrust faults in southern Mexico and interpret this deformation as evidence that Caribbean–North America Plate motion steps northward into southern Mexico and dies out before it reaches the Middle America trench.

## 3 GPS DATA AND PROCESSING METHOD

The GPS velocities used in our analysis are determined from measurements we made at 32 campaign stations in Honduras and four campaign stations in areas of El Salvador, and publicly available data from continuous stations TEGU in Honduras and GUAT in Guatemala (Table 1 and Fig. 4). Measurements at four stations in eastern Honduras began in 2000 and are described by DeMets *et al.* (2007). Measurements at the remaining campaign sites began in 2003 and 2004 (Table 1) and consist of daily 24-hr occupations that lasted for 1–16 d per station for each occupation. All of the campaign measurements were made using Trimble 5700 GPS receivers and Zephyr geodetic antennas except a handful of sites that were occupied in 2005 with Trimble 4000 receivers and Trimble choke ring

antennas. All antennas were mounted on 0.55 m high, precisely levelled spike mounts, thereby eliminating incorrect antenna heights as a source of spurious antenna phase centre offsets.

All of the continuous and campaign GPS data used in this study were processed with GIPSY software from the Jet Propulsion Laboratory (JPL). The daily data from individual GPS sites were initially processed using a precise point-positioning strategy (Zumberge *et al.* 1997), after which the daily station solutions were combined to resolve phase ambiguities using Ambizap software (Blewitt 2008). The daily site coordinates were first estimated in a no-fiducial reference frame from fiducial-free satellite orbits and satellite clock corrections from JPL (Heflin *et al.* 1992), after which they were transformed to ITRF2005 (Altamimi *et al.* 2007) using daily seven-parameter Helmert transformations from JPL.

We reduced scatter in the estimated daily locations of each GPS site by using the time-series of well-behaved, continuous stations within and external to our study area to estimate and remove common-mode noise from the daily station coordinates (Marquez-Azua & DeMets 2003). The repeatabilities of the north and east components of the daily station coordinates are 2–3 and 3–5 mm, respectively, after correcting for common-mode errors. Station velocities were estimated via linear regression of the corrected station coordinates (Figs 5 and 6) and velocity uncertainties were determined with an empirically derived error model that accounts for

**Table 1.** GPS station information.

| Site name | Coordinates | | Station days | | | | | Velocity[a] | |
|---|---|---|---|---|---|---|---|---|---|
| | Lat. (N) | Long. (E) | 2003 | 2004 | 2005 | 2006 | 2007 | North | East |
| CEGD | 13.9395 | −88.9017 | – | 7 | 7 | 7 | 11 | 6.9 ± 0.7 | 9.9 ± 1.2 |
| CARI | 13.8333 | −87.6891 | – | 3 | – | 6 | 4 | 5.2 ± 1.4 | 7.9 ± 1.1 |
| CHIQ | 14.2820 | −87.5091 | 7 | – | 4 | 1 | 3 | 5.9 ± 1.4 | 8.1 ± 1.5 |
| CMP1 | 14.5092 | −85.7146 | – | – | 2 | – | – | 6.4 ± 1.8 | 11.3 ± 2.8 |
| CNCH | 14.0269 | −88.3438 | – | 3 | – | 3 | 3 | 7.1 ± 2.9 | 7.4 ± 4.6 |
| ECOP | 15.3318 | −88.3236 | – | 7 | 1 | 3 | – | 7.3 ± 5.0 | 6.1 ± 7.7 |
| ERAN | 14.2321 | −88.4634 | – | 4 | – | 3 | 3 | 6.6 ± 2.8 | 7.4 ± 4.4 |
| ERAZ | 14.6014 | −87.1136 | – | 7 | – | 4 | 5 | 4.9 ± 1.0 | 9.1 ± 2.2 |
| FRT1 | 15.7797 | −88.0401 | – | 7 | 3 | – | 5 | 3.1 ± 2.8 | 3.9 ± 4.0 |
| GLCO | 15.0298 | −86.0699 | – | 3 | – | – | – | 7.1 ± 2.7 | 14.8 ± 4.3 |
| GRAC | 14.5885 | −88.5843 | – | 3 | 1 | 3 | 3 | 6.9 ± 3.6 | 8.8 ± 5.8 |
| GUAJ | 14.2283 | −89.4687 | – | 9 | 7 | 8 | 7 | 4.9 ± 0.6 | 7.5 ± 0.9 |
| GUAT | 14.5904 | −90.5202 | 288 | 326 | 343 | 348 | 345 | 2.8 ± 0.5 | 3.8 ± 1.0 |
| JAGU | 15.0991 | −88.7099 | – | 6 | 4 | – | 4 | 5.9 ± 1.0 | 6.0 ± 1.1 |
| LCAN | 14.7303 | −88.4371 | – | 3 | 3 | – | 4 | 5.6 ± 2.8 | 8.2 ± 4.5 |
| LCEB | 15.7479 | −86.8407 | – | 5 | 2 | – | 4 | 5.7 ± 2.5 | 7.6 ± 3.5 |
| LESP | 14.3148 | −88.1605 | – | 13 | – | 4 | 3 | 5.0 ± 2.4 | 7.1 ± 3.2 |
| LJAS | 13.5957 | −87.7470 | – | 7 | – | 5 | 7 | 5.0 ± 1.0 | 8.2 ± 1.1 |
| LPZW | 14.3138 | −87.6909 | 6 | – | 6 | 7 | 5 | 4.9 ± 0.7 | 7.9 ± 1.4 |
| MAYA | 14.8406 | −89.1346 | – | 3 | 1 | – | 4 | 5.5 ± 3.2 | 6.5 ± 4.3 |
| MEZA | 15.4452 | −87.9311 | 16 | – | 3 | – | 6 | 5.8 ± 2.1 | 6.0 ± 3.0 |
| MNGO | 13.9651 | −89.1974 | – | 6 | 7 | 7 | 17 | 7.3 ± 0.6 | 8.7 ± 1.0 |
| MNTO | 14.9167 | −86.3805 | – | 3 | – | – | – | 7.7 ± 2.2 | 13.4 ± 4.5 |
| MORO | 13.5989 | −86.9246 | – | 3 | – | 4 | 4 | 6.0 ± 1.0 | 6.1 ± 2.0 |
| NAJO | 15.5569 | −87.6249 | – | 8 | 3 | – | – | 4.7 ± 6.6 | 6.6 ± 8.9 |
| NDAM | 13.6777 | −87.3568 | – | 6 | – | 3 | 4 | 5.1 ± 2.9 | 8.5 ± 4.0 |
| NOCO | 14.4384 | −89.1987 | – | 11 | 3 | 5 | 4 | 11.5 ± 0.9 | 10.0 ± 1.0 |
| OCOM | 14.6951 | −87.9491 | – | 3 | 7 | – | 4 | 6.9 ± 2.7 | 7.8 ± 3.9 |
| OSIC | 13.8139 | −88.1457 | – | 8 | 7 | 7 | 8 | 6.0 ± 0.7 | 10.4 ± 1.1 |
| RECA | 13.3322 | −87.1548 | – | 6 | – | 10 | 3 | 5.1 ± 2.6 | 8.4 ± 3.7 |
| ROSA | 14.7669 | −88.7757 | – | 3 | 3 | – | 4 | 5.4 ± 3.0 | 8.4 ± 4.2 |
| SFDP | 14.9659 | −86.2449 | – | 3 | – | – | – | 6.0 ± 2.2 | 12.3 ± 3.7 |
| SGTO | 13.0995 | −87.0626 | – | 3 | – | 5 | 4 | 4.7 ± 1.7 | 5.0 ± 1.6 |
| SJAN | 14.8152 | −88.2111 | – | 3 | 5 | – | 2 | 7.6 ± 2.9 | 7.4 ± 4.0 |
| SNTA | 14.0663 | −87.9502 | – | 3 | – | 5 | 4 | 6.0 ± 1.3 | 9.3 ± 1.7 |
| TEGU | 14.0901 | −87.2056 | 235 | 366 | 323 | 58 | 189 | 4.3 ± 0.5 | 7.9 ± 0.8 |
| TONU | 13.9260 | −86.8407 | – | 6 | – | 3 | 4 | 5.3 ± 3.8 | 9.2 ± 4.3 |

[a]Velocities are relative to ITRF05 and are specified in units of millimetres per year. Uncertainties are standard errors. Information about station histories before 2003 is given by DeMets *et al.* (2007).

different noise components in the time-series (white noise, flicker noise and random monument walk) (Mao *et al.* 1999).

For the tectonic analysis below, all GPS station velocities were transformed from ITRF2005 to a Caribbean Plate reference frame using an angular velocity that best fits the ITRF2005 velocities that we determined for 17 GPS stations on the Caribbean Plate (locations shown in Fig. 1). These 17 stations include all 15 Caribbean Plate sites that were used by DeMets *et al.* (2007) to estimate Caribbean Plate motion and two newer stations, BDOS on Barbados and HOUE on Guadeloupe. Only four stations from the study area, all in undeforming areas of eastern Honduras (sites CMP1, GLCO, MNTO and SFDP in Fig. 4), were used to estimate the best-fitting Caribbean Plate angular velocity (DeMets *et al.* 2007). All of the other stations from the study area are located within actively deforming areas of Central America and are thus unsuitable for estimating the Caribbean Plate angular velocity.

The best-fitting angular velocity for the motion of the Caribbean Plate relative to ITRF2005 is 37.8°N, 98.5°W, 0.262° Myr$^{-1}$. The uncertainties in this angular velocity are propagated rigorously into our station velocity uncertainties and typically increase the standard

error in the station velocity uncertainties by 0.2 mm yr$^{-1}$ or less. Relative to the much larger uncertainties that are characteristic of our station velocities (Table 1), the additional reference frame uncertainty is too small to affect any aspect of the ensuing analysis. We suspect that our estimates of the site velocity uncertainties are overly pessimistic given that the campaign site velocities exhibit a significantly greater degree of consistency with each other (Fig. 4) and with the well characterized velocities of the continuous stations TEGU and SLOR (Fig. 6) than might be expected if their estimated uncertainties were correct.

## 4 GPS VELOCITY FIELD

We next describe the GPS station velocities relative to the Caribbean Plate reference frame (Fig. 4), beginning at the eastern end of the Honduran network and proceeding west through zones 3, 2b, 2a and 1 as defined by Rogers & Mann (2007). We exclude campaign site NOCO in westernmost Honduras from our analysis since its motion is anomalous with respect to other nearby stations (Figs 5 and 4).
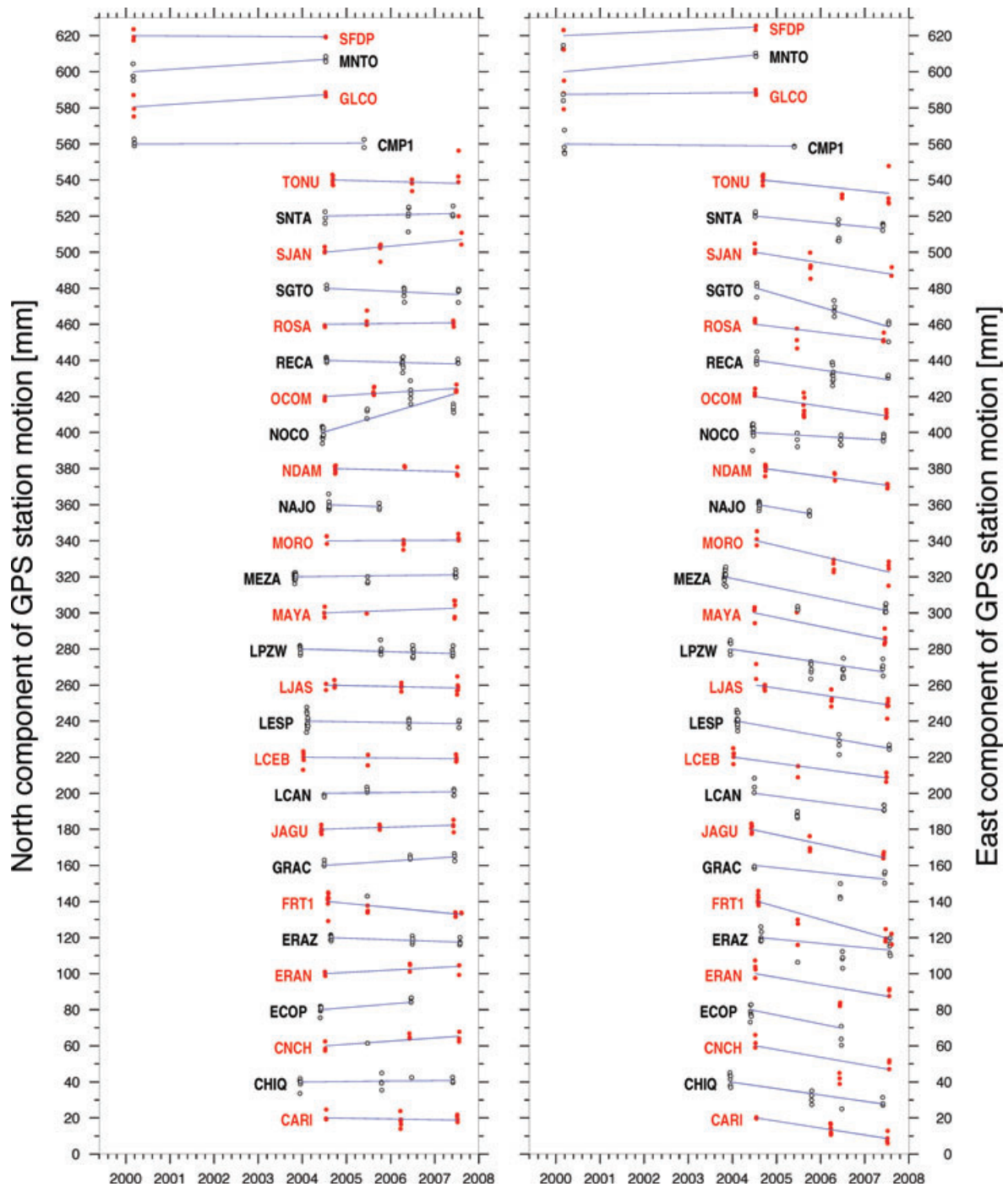
**Figure 5.** Horizontal components of the GPS coordinate time-series for campaign stations. Red circles show site locations determined from daily 12- to 24-hr-long sessions. Blue lines are best fitting lines determined from linear regressions of the station coordinate time-series. Station motions are relative to the Caribbean Plate.

The geodetic pin at this site is epoxied into a 3 m radius, rounded boulder that floats in valley alluvium and may be unstable.

### 4.1 Zones 3 and 2b of eastern Honduras

Only four stations are located in zones 2b and 3 of eastern Honduras (Fig. 4), where Rogers & Mann (2007) find no geomorphologic evidence for active faulting or extension. All four stations have motions insignificantly different from zero within their uncertainties, as re-

ported by DeMets *et al.* (2007). We conclude that stable areas of the Caribbean Plate extend as far west as zone 2b, in accord with the absence of any geomorphologic or seismic evidence for active faulting in this region (Fig. 7).

### 4.2 Zone 2a of central Honduras

All six stations that are located east of or close to the Honduras Depression within or near zone 2a (blue arrows in Fig. 8) move
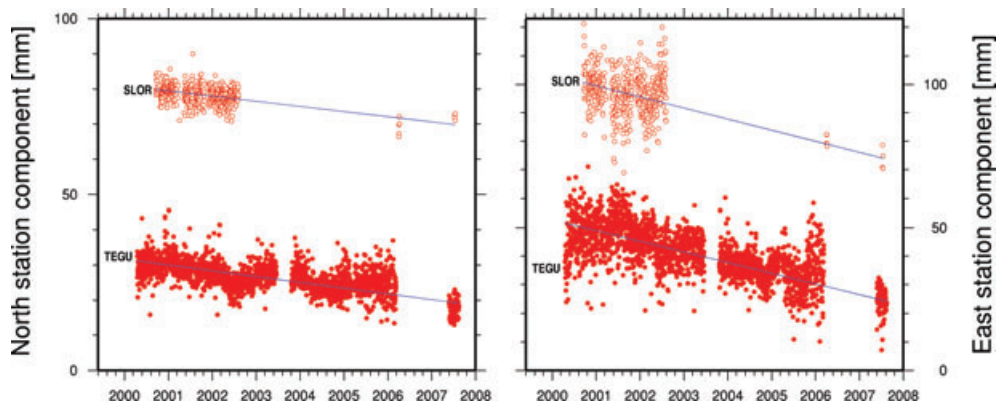
**Figure 6.** Horizontal components of continuous GPS coordinate time-series. Station motions are relative to the Caribbean Plate.
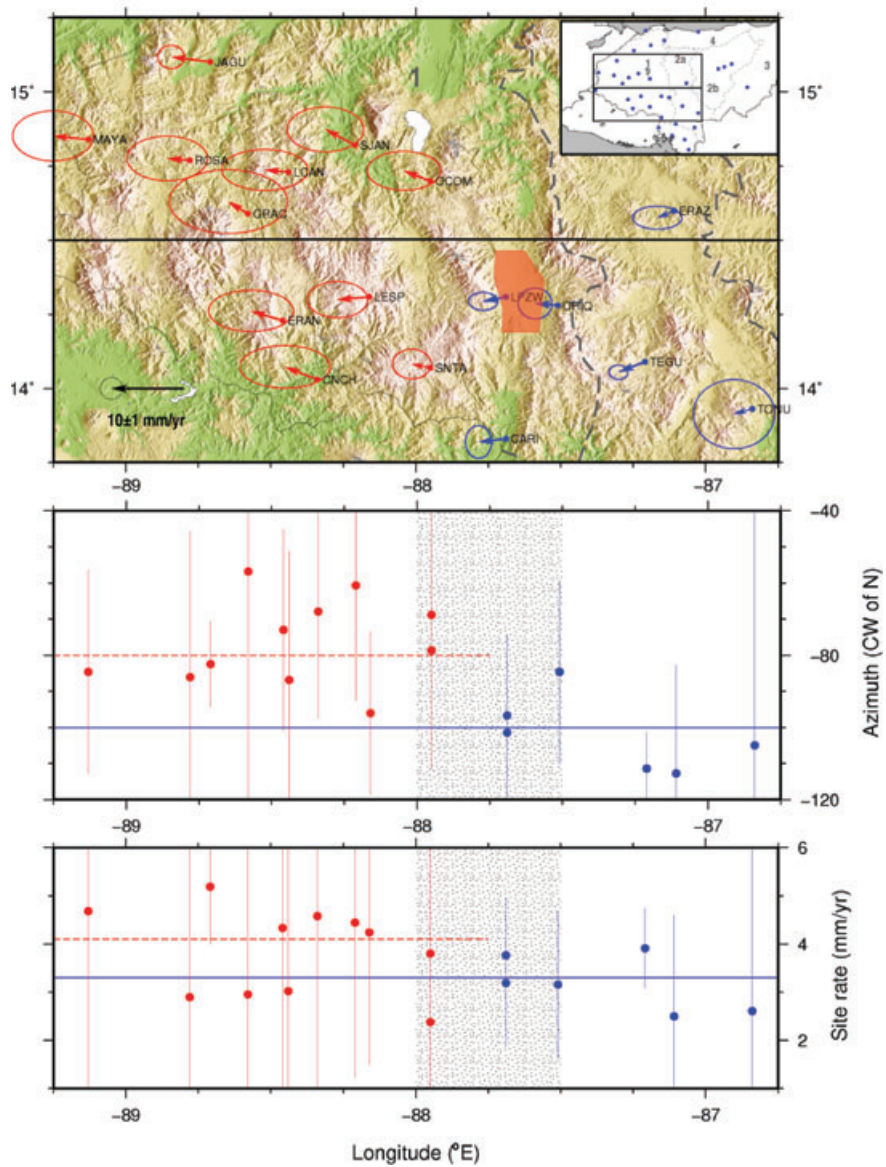


**Figure 7.** Upper panel: GPS site motions in central Honduras relative to the Caribbean Plate. Uncertainty ellipses are 2-D, $1\sigma$. Dashed lines indicate the zone boundaries from Fig. 4. Middle panel: GPS station directions from upper image versus station longitude. Uncertainties are 1-D, $1\sigma$. The blue and red horizontal lines show the weighted, average directions determined from the directions of stations with blue and red symbols in the upper image. Stippled region approximates the transition zone where a change in velocities occurs and corresponds with the eastern limit of the seismicity in Honduras (also see Fig. 7). Lower panel: longitudinal transect with GPS station rates from the upper image and weighted, average rates (blue and red horizontal lines).
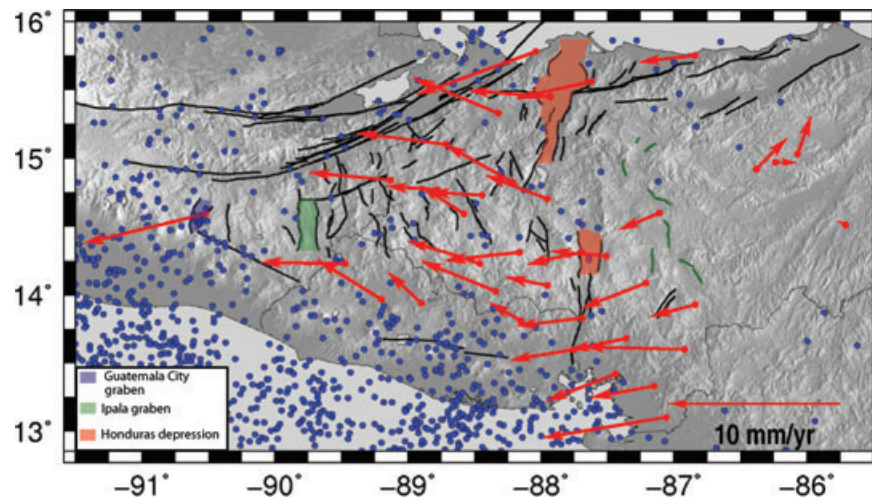
**Figure 8.** GPS site velocities relative to Caribbean Plate with topography and known faults. Blue circles are epicentral locations for 1973–2008 earthquakes with $M_{\rm w} \geq 3$ and depths above 50 km from the National Earthquake Information Center. The subtle change in GPS velocities shown in Fig. 8 and described in the text coincides with the approximate eastern limit of seismicity in Honduras.

to the west, away from the plate interior. Their average westward rate is $3.3 \pm 0.6$ mm yr$^{-1}$ (all uncertainties quoted hereafter are $1\sigma$), indicating that their motion away from the Caribbean Plate interior is significant at high confidence level. By implication, the western limit of stable parts of the Caribbean Plate is east of stations ERAZ, TEGU and TONU in central Honduras. Additional stations in zones 2a, 2b and 3 are needed to determine more precisely where the stretching begins.

### 4.3 Zone 1: possible transition across the Honduras Depression

A second change in station velocities may occur across the Honduras Depression (Fig. 8), roughly coinciding with the eastern boundary of the active rift province of western Honduras (zone 1). Without exception, the stations in zone 1 move to the west-northwest (shown by red arrows in Fig. 8). Their $4.1 \pm 0.6$ mm yr$^{-1}$ average rate is faster than the $3.3 \pm 0.6$ mm yr$^{-1}$ average rate for sites in zone 2a, though not significantly so. A $\approx 20°$ clockwise change in the site directions also occurs between zone 2a and zone 1, from an average of S79°W $\pm$ 8° at locations within and east of the Honduras Depression to N80°W $\pm$ 9° at locations farther west (Fig. 8). The change in station motions is consistent with slow extension ($\sim$1 mm yr$^{-1}$) across the Honduras Depression and also coincides with the eastern limit of seismicity in Honduras (Fig. 7).

### 4.4 From zone 1 to Guatemala

Between zone 1 in western Honduras and station GUAT, which is located in the Guatemala City graben, the rate of westward station motion increases from $4.1 \pm 0.6$ mm yr$^{-1}$ in western Honduras to $7.3 \pm 1.1$ mm yr$^{-1}$ at GUAT (Fig. 4). The $3.2 \pm 1.3$ mm yr$^{-1}$ difference between these two rates represents the combined extension rate across the Ipala graben of southern Guatemala (Fig. 4) and the eastern bounding fault of the Guatemala City graben. The extension rate we estimate at station GUAT, $7.3 \pm 1.1$ mm yr$^{-1}$, agrees with previously published estimates (8 mm yr$^{-1}$) for station GUAT (Lyon-Caen *et al.* 2006; DeMets *et al.* 2007). Geodetic evidence for

an additional 3–4 mm yr$^{-1}$ of extension west of Guatemala City is described by Lyon-Caen *et al.* (2006).

### 4.5 Other areas: the Gulf of Fonseca

A possibly significant variation in the velocity field also occurs in southern Honduras and eastern El Salvador around the Gulf of Fonseca (green arrows in Fig. 4), where stations move uniformly to the west–southwest, similar to stations in zone 2a, but at modestly faster rates ($4.6 \pm 1$ mm yr$^{-1}$). These station motions are poorly fit by the series of finite element models that we describe below. Further modelling and observations from this region are needed to better understand the cause(s) of the westward motions of these sites.

### 4.6 Velocity field synthesis

In summary, the rate of westward motion across the 400-km-wide extending zone in Honduras and southern Guatemala increases systematically from east to west, with insignificant motion of $0 \pm 1$ mm yr$^{-1}$ in the tectonically inactive zones 3 and 2b, westward motion of $3.3 \pm 0.6$ mm yr$^{-1}$ in zone 2a, WNW-directed motion of $4.1 \pm 0.6$ mm yr$^{-1}$ in zone 1, westward motion of $7.3 \pm 1.1$ mm yr$^{-1}$ in the Guatemala City graben, and motion of 11–12 mm yr$^{-1}$ at locations west of the Guatemala City graben. Active extension is thus widely distributed across Honduras and Guatemala, with one-third of the total extension in Honduras and the remainder in southern Guatemala. Measurements at additional stations in some areas and continued measurements at the existing stations are underway to better establish how much motion occurs across individual grabens.

## 5 FINITE ELEMENT MODELLING ASSUMPTIONS AND CONFIGURATIONS

Our modelling objective is to identify the simplest geologically reasonable model that successfully captures the major aspects of the GPS velocity field in northern Central America. To achieve this goal, we explore two groups of FEMs. The first series of models,

which are described in Section 6.1, is used to isolate the effects of different, idealized fault geometries and driving conditions on long-term deformation in the study area. The second, which is described in Section 6.2, consists of FEMs that approximate the fault geometry in northern Central America and use the well-determined relative motion between the Caribbean and North American Plates to drive the model. Both sets of FEMs incorporate three key features of the study area. Each incorporates a continuous strike-slip fault that approximates the Swan Island and Motagua faults. Each includes a northwest-trending mesh boundary to simulate the Middle America trench as it converges diagonally with the strike-slip plate boundary. Finally, each includes a crustal weak zone parallel to the Middle American trench in order to simulate the rheologically weak Central America volcanic arc.

## 5.1 Specifics of the mesh and driving conditions

We use the finite-element code ABAQUS (version 6.4) to construct all of the 3-D finite-element models (FEMs). The models consist of 8-node linear brick elements and impose values of 0.25 for Poisson's ratio and 75 GPa for Young's modulus, the only elastic parameters necessary for our modelling. Following ten Brink *et al.* (1996), the crust is modelled as a 15-km-thick elastic layer that we further subdivide into 3-km-thick layers. Our model approximates the influence of the upper mantle and lower crust on the long-term deformation of the upper crust via steady driving at known plate velocities of some of the nodes that define the base of our mesh (described in next section).

Strike-slip faults in the models are represented by vertical faults that cut entirely through the mesh. The strike-slip faults are modelled as free-slip boundaries along which the nodes that define the fault are required to move horizontally and parallel to the fault surface. We did not attempt to incorporate the elastic effects of frictional coupling across any strike-slip faults, mainly because only one of our GPS stations (station FRT1) is close enough to the plate boundary faults to experience significant elastic effects from them. We also ignore the possible elastic effects of the many graben-bounding faults that may be active in our study area, which we assume are insignificant given the likely slow motion across any single graben.

A no-displacement condition is imposed on all faces of the mesh that define the edges of fixed blocks. Other mesh edges are allowed to displace horizontally, thereby simulating long term plate motion along the faults that cut through the model.

Following the lead of ten Brink *et al.* (1996), we drive deformation of our FEMs by imposing the known plate motion on the basal nodes beneath areas that are prescribed to move as an undeforming block. In all other areas, the mesh nodes are permitted to move freely. This approach permits us to define areas of the mesh where deformation can occur and to preclude deformation in areas of the mesh that correspond to areas where there is no geological or other evidence for long-term surface deformation.

## 5.2 Mesh validation

We validated the approach outlined above using a simple rectangular mesh that consists of two blocks separated by a curved strike-slip fault (Fig. 9). We fixed the edges of one block and required a subset of the basal nodes beneath the second block to rotate around the same pole that was used to define the curved fault. The moving nodes therefore trace out small circles that are parallel to the curved

fault. The rates of motion prescribed for the nodes increase linearly with their distance from the pole, as would a rigid block that rotates in a plane. The driving constraints are imposed on all basal nodes farther than 50 km from the fault. All nodes within 50 km of the fault are allowed to move freely and thus accumulate deformation.

Calculations with this FEM for a unit offset of the basal nodes yield no strain at any location in the mesh. This agrees with our expectation that no long-term strain should accrue in the crust adjacent to an unlocked fault that accommodates pure strike-slip motion. This validates our approach and sets the stage for the modelling results that are described in the following section.

## 5.3 Comparison of assumptions to Alvarez-Gomez *et al.* (2008)

Our modelling approximations and boundary constraints are similar to many of those used by Alvarez-Gomez *et al.* (2008). These include the approximate configuration and geometries of the primary plate boundary faults that are embedded within our meshes, the assumption of a homogeneous elastic crust except for the rheologically weak Central America volcanic arc, the constraint of strike-slip motion along the Motagua fault, and the assumption that the Motagua fault accommodates most or all of the strike-slip component of present plate motion, as suggested by GPS measurements from Guatemala (Lyon-Caen *et al.* 2006).

Two differences between our modelling approaches merit brief discussion. First, Alvarez-Gomez *et al.* (2008) explicitly model the degree of frictional coupling along the Middle America subduction interface to assess its potential influence on deformation within the overlying Caribbean Plate. They conclude that any frictional coupling across the subduction interface is weak or non-existent and thus has little or no influence on deformation of the upper plate. Independent GPS measurements at coastal stations in Nicaragua (Turner *et al.* 2007), Guatemala (Lyon-Caen *et al.* 2006) and El Salvador (Alvarado 2008; Correa-Mora *et al.* 2009) reveal no evidence for significant frictional coupling across the subduction interfaces offshore from these countries and therefore corroborate Alvarez-Gomez *et al.*'s conclusion. Based on these results, we allow the nodes that approximate the Middle America subduction interface to respond freely to deformation in the rest of the mesh, corresponding to a frictionless boundary condition on that feature.

Our approaches to driving deformation of our FEMs also differ. Alvarez-Gomez *et al.* (2008) impose Caribbean Plate motion in their FEM by pulling along a vertical node-plane that lies in the Caribbean Sea ~800 km east of the study area. We instead use basal drag to drive Caribbean Plate motion in all but one of our FEMs. This approach has two advantages. First, the motions of the basal nodes that are located close to the deforming areas of northern Central America provide more realistic driving conditions for deformation in those areas than do the motions of edge nodes that are located in the Caribbean Sea hundreds of kilometres east of the deforming area. Second, deformation of the mesh can be limited to areas where it is known to occur via appropriate selection of the basal nodes that are used to drive the model. We show below that a mesh that is driven by pulling on nodes that are located hundreds of kilometres east of the study area predicts significant stretching in areas of eastern Honduras where geological data and GPS measurements show no evidence for active deformation (Rogers *et al.* 2002; DeMets *et al.* 2007).
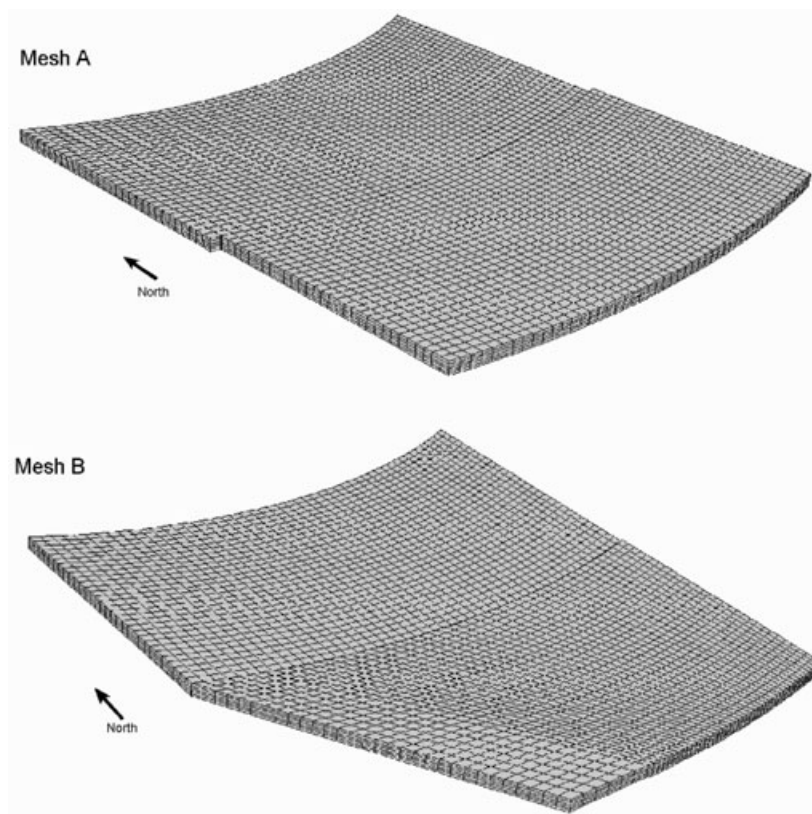
**Figure 9.** Idealized finite element meshes described in the text. Mesh A depicts a model with a curved strike-slip fault that cuts entirely through the mesh from side to side and top to bottom. Mesh B depicts the same mesh, but simulates the obliquely intersecting Middle America trench and Caribbean–North America strike-slip plate boundary.

## 6 RESULTS

### 6.1 Idealized meshes

We first explore the deformation patterns for three idealized FEMs that simulate important tectonic features of northern Central America. The simplest of the three FEMs incorporates a curved strike-slip fault that offsets a rectangular mesh (mesh A of Figs 9 and 10a). The second FEM approximates the wedge-shaped geometry of the western end of the Caribbean Plate (mesh B of Figs 9 and 10b). The third FEM includes a narrow weak zone to simulate the expected rheological behaviour of the volcanic arc (Fig. 10c). The boundary constraints and fault slip conditions that we apply to all three FEMs are specified in Section 5.1.

Deformation of the three meshes is induced by imposing an eastward, unit displacement of the southern basal nodes that are located more than 50 km from the curved strike-slip fault, thereby simulating the motion of the southern block about a distant pole of rotation (Fig. 10). The nodes within 50 km of the curved strike-slip fault are allowed to move freely and hence deform, subject to the constraint of strike-slip motion for the nodes that define the fault. Confining deformation to locations within 50 km of the fault enhances the pattern of strain near the fault and is done merely for convenience. Models in which we move only the southernmost row of nodes to the east result in a similar but more diffuse pattern of strain within the southern block, with strain magnitudes decreasing with distance from the curved fault.

Fig. 10(a) shows the pattern of principal strain-rates for the first of the three FEMs. The nodes that define the strike-slip fault accom-

modate free slip along the fault via their fault-parallel component of motion, leaving their fault-perpendicular component of motion to induce strain within the areas near the fault. Fault-normal shortening is thus predicted in areas where the curved fault trace resists the basal flow and fault-normal extension in areas where the residual component of motion is directed away from the fault. As expected, the predicted strain rates are small for areas where the fault trend lies within a few degrees of E–W, but become progressively larger as the angle between the local strike of the fault and the eastward crustal motion increases.

Fig. 10(b) shows strain rates calculated for the FEM with a wedge-shaped geometry along the western side of its southern block. The pattern of strain differs from that for the first FEM only within the narrow, western part of the wedge, where the strain-rate magnitudes are smaller and the strain-rate axes are rotated anticlockwise from their counterparts in the first model. The wedge-shaped mesh geometry thus only causes localized changes in predicted strain rates.

The pattern of strain predicted for the third FEM (Fig. 10c), which simulates the rheology of the Central America volcanic arc by incorporating a trench-parallel zone with a Young's modulus that is one order of magnitude lower than for the rest of the model (7.5 GPa versus 75 GPa), differs only modestly from that for the simpler wedge-shaped model (Fig. 10b). The principal strain rates near the intersection of the weak zone with the strike-slip fault are smaller in magnitude and rotated anticlockwise relative to those for the second FEM. The weak zone thus only locally modifies the magnitudes and orientations of the principal strain rates.

Despite their differences, all three of the idealized FEMs predict that the orientations of the principal strain-rate axes change
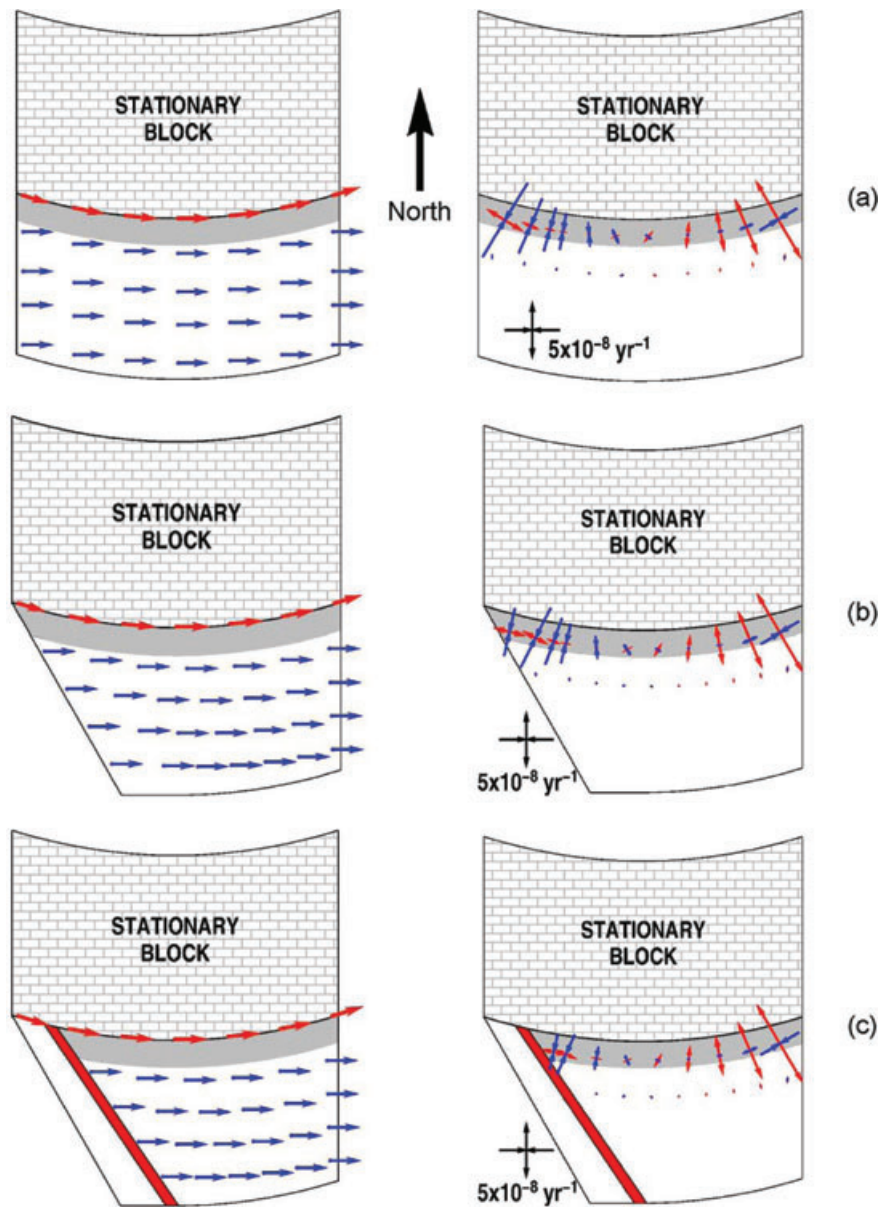
**Figure 10.** Left-hand column: fault geometries and driving constraints for three idealized FEMs described in the text. Blue arrows indicate displacements that are imposed on nodes at the base of the mesh. Red arrows indicate strike-slip constraint that is imposed on the motions of all nodes that define the curved strike-slip fault. Shaded region adjacent to the fault is allowed to deform freely, subject to the condition of strike-slip motion along the fault. The diagonal red bands in the FEMs in the lower row are low-strength zones that simulate a weak volcanic arc. Right-hand column: principal strain rates predicted by each FEM in response to the eastward motions of the basal nodes. The principal shortening and stretching strain-rate axes are shown by the blue and red arrows, respectively.

significantly (~90°) along the fault. At the western end of the deforming region, the principal strain-rate axes are extensional and are oriented ~E–W, nearly parallel to the fault. At locations where the fault azimuth and basal driving direction are similar, little or no strain is predicted, as expected. At the eastern end of the fault, all three FEMs predict that fault-perpendicular stretching occurs. These results agree qualitatively with evidence described by Rogers & Mann (2007) for a significant change in the principal direction of extension south of the Motagua and Swan Islands faults from E–W extension across grabens in southern Guatemala to NNW–SSE extension along prominent, boundary-parallel normal faults that offset sediments offshore from northern Honduras. Modifications to the idealized meshes to simulate the wedge-shaped geometry of the

study area and incorporate a weak volcanic arc (Figs 10b and c) do not significantly alter this result. We conclude that the orientation and curvature of the idealized fault with respect to the direction of the basal driving motion strongly influence the pattern of strain.

## 6.2 FEMs that simulate northern Central America tectonics

### 6.2.1 Model specifications

We assess the fits of twelve alternative FEMs to the Honduran and Salvadoran GPS station velocities (Fig. 4). All of the FEMs employ the same mesh, which consists of 53 875 8-node linear brick
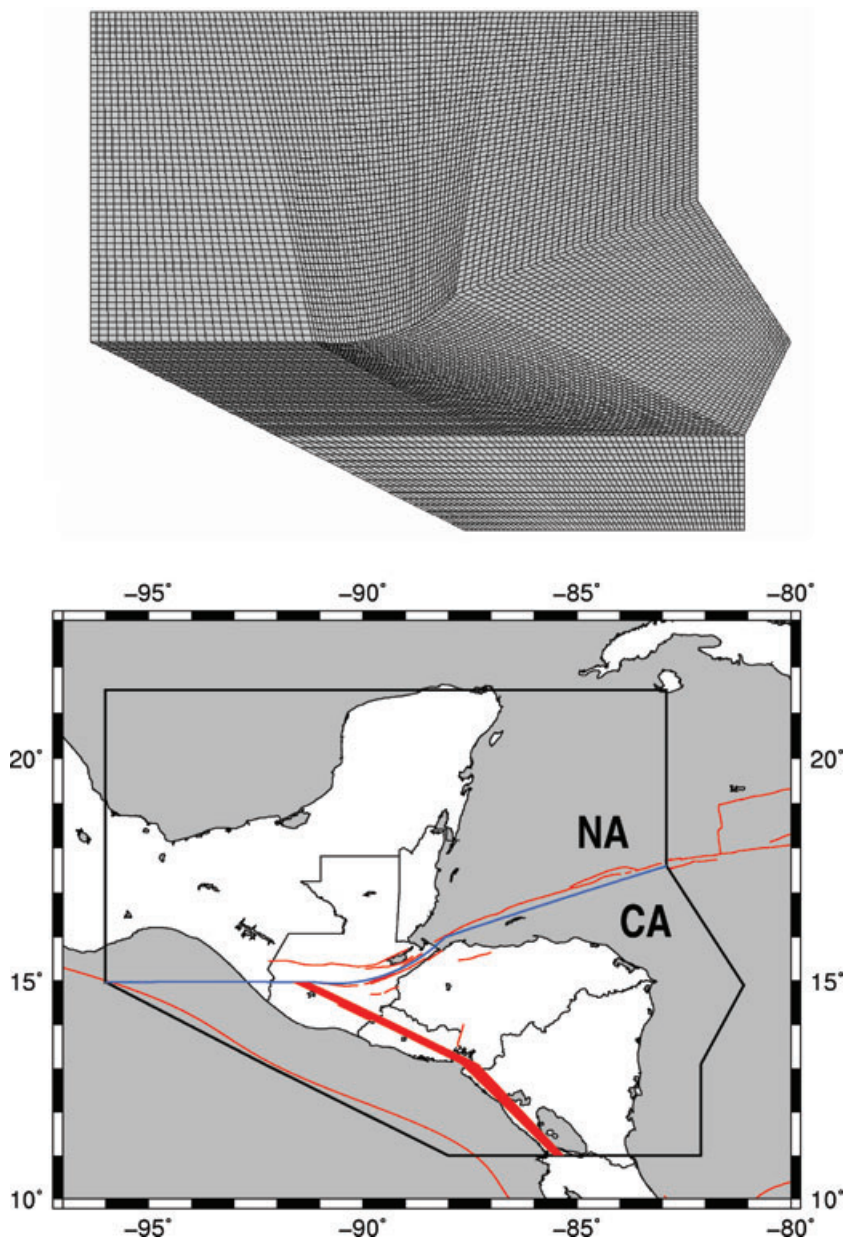
**Figure 11.** Upper panel: finite element mesh used to model deformation of northern Central America. Lower panel: overlay of mesh boundaries and faults on the western end of the Caribbean Plate. Red lines show the actual locations of the major faults and volcanic arc. Blue line shows the mesh boundary that is used to simulate the Caribbean–North America Plate boundary. 'NA' is North American Plate and 'CA' is Caribbean Plate.

elements that comprise 66 528 nodes (Fig. 11). The mesh elements within our study area have approximate horizontal dimensions of 10 km, sufficiently dense for our purposes. A uniform 15-km-elastic layer depth is used throughout the mesh. The mesh is constructed in geographic coordinates, but employs a flat Earth approximation. Simple calculations suggest that this approximation is unlikely to cause artefacts in the predicted deformation larger than a few tenths of a millimetre per year.

Ten of the twelve FEMs described below model the boundary between the North American and Caribbean Plates as a freely slipping, through-going strike-slip fault whose trace approximately follows the Swan Islands fault and Motagua fault (Fig. 11). The other two FEMs use a straight plate boundary fault in Central America for the purpose of documenting the influence of a curved versus a straight plate boundary on the model predictions.

In all 12 models, the North American Plate is fixed and displacement is imposed along either the basal or edge nodes of the Caribbean Plate. The motion at each node is calculated using an angular velocity for Caribbean–North America Plate motion (74.1°N, 204.0°E, 0.190° Myr$^{-1}$) that we determined from an inversion of the velocities of 17 Caribbean Plate GPS stations (locations shown in Fig. 1) and ~650 continuous stations from stable parts of the North American Plate (not shown). The motion predicted by this updated angular velocity differs insignificantly (by tenths of a millimetre per year and tenths of a degree) from that predicted by the Caribbean–North America Plate angular velocity of DeMets *et al.* (2007), which is based on shorter GPS time-series and the older ITRF2000 geodetic reference frame. Once the FEM calculations of the surface node velocities are complete, we subtract the motion predicted for the Caribbean Plate at each node from its calculated

**Table 2.** Finite element model characteristics.

| Model | Deformation constraint on connection to MAT[a] | Driving constraint[b] | Young's modulus for volcanic arc in GPa[c] |
|---|---|---|---|
| CA101 | Free | Areas > 50 km from fault | 7.5 |
| CA102 | Free | Nodes in and east of central Honduras | 7.5 |
| CA103 | Free | Nodes east of central Honduras | 7.5 |
| CA103P | Pinned | Nodes east of central Honduras | 7.5 |
| CA104 | Free | Eastern edge of mesh[d] | 7.5 |
| CA104P | Pinned | Eastern edge of mesh[d] | 7.5 |
| CA105 | Free | Nodes east of central Honduras | 75[e] |
| CA106 | Free | Nodes east of central Honduras | 0.75 |
| CA107 | Free | Nodes east of central Honduras | 30 |
| CA108 | Free | Nodes east of central Honduras | 7.5[f] |
| CA203[g] | Free | Nodes east of central Honduras | 7.5 |
| CA203P[g] | Pinned | Nodes east of central Honduras | 7.5 |

[a]Specifies whether the plate boundary fault that connects the western end of the Motagua fault to the Middle America Trench (MAT) is free to slip or pinned. Pinning the fault forces deformation to occur over a broad zone.

[b]Specifies where Caribbean–North America Plate motion is imposed on the basal or edge nodes of the model. See also Fig. 12.

[c]Specifies strength that is used to simulate the volcanic arc. Young's modulus for areas of the model other than the volcanic arc has an assigned value of 75 GPa.

[d]Simulates driving condition applied by Alvarez-Gomez *et al.* (2008).

[e]Mesh is elastically homogeneous since Young's modulus for the volcanic arc (75 GPa) is the same as for the rest of the model.

[f]Width of the assumed weak zone reduced by 50 per cent.

[g]Adopts straight plate boundary trace in Central America (Fig. 16).

velocity, thereby changing the frame of reference to the Caribbean Plate.

Table 2 specifies the configurations of all 12 FEMs that we explored and Fig. 12 shows the fault geometries, driving conditions, and fits of most of these models. Models CA101 to CA104 test the effect of four different sets of driving conditions on FEMs with identical fault and mesh geometries. Models CA105–CA108 are used to determine how different assumed strengths for the volcanic weak zone affect the fit to the GPS velocity field. We also explore the fits of models in which Caribbean–North American Plate motion west of the Central American volcanic arc is accommodated across a wide deformation zone, as proposed by Burkart (1983) and Guzman-Speziale *et al.* (1989). We enforce this wider deformation zone by employing a technique described by Alvarez-Gomez *et al.* (2008), namely, we pin the strike-slip fault west of the volcanic arc to preclude slip along that feature. Since this constitutes a simple modification of models CA103 and CA104, these modified models are named CA103P and CA104P. Finally, we describe the fits of models CA203 and CA203P, which employ the same driving conditions as models CA103 and CA103P, but incorporate a straight trace instead of curved trace for the Motagua fault. The latter two models establish how the curved trace of the Motagua fault influences the predicted deformation field.

### 6.2.2 Model fits

The goodness-of-fit for each FEM is measured using the $\chi^2$ statistic, where $\chi^2$ is the summed least-squares difference between the predicted and measured velocities at each GPS site divided by the velocity uncertainty. None of the FEM calculations include the anomalous GPS velocity at site NOCO or the velocity at station GUAT, for which the fit is discussed separately.

Model CA101 imposes Caribbean Plate motion on nearly all of the basal nodes beneath our study area, including many nodes that are located beneath areas of central and western Honduras where active extension occurs (see inset CA101 in Fig. 12). Because

deformation of the mesh cannot occur above areas where the basal nodes are prescribed to move at the plate rate, this model poorly fits the velocities of GPS stations that are located in deforming areas of Honduras (Fig. 12). Its cumulative least-squares misfit is more than twice as high as the best models we explored.

Model CA102 imposes Caribbean Plate motion on the basal nodes between the eastern limit of our mesh and the Honduras Depression in central Honduras (see inset CA102 in Fig. 12). It thus permits active deformation to occur in parts of the mesh that correspond to western Honduras and some of central Honduras. This model reduces the least-squares misfit by ∼25 per cent relative to the misfit for model CA101, but predicts GPS station velocities that are consistently 15–70° clockwise from the measured velocities (compare blue and red velocities in upper panel of Fig. 13).

The poor fits of models CA101 and CA102 illustrate that models that restrict deformation to too small of a region south of the Motagua fault cannot fit the GPS velocity field given the other constraints and assumptions that are embedded in our FEMs. We thus next examine the fits of models that permit deformation to occur across increasingly wide parts of Central America and the Caribbean Sea.

In model CA103, Caribbean Plate motion is imposed on the basal nodes between the eastern edge of the mesh and eastern Honduras (see inset CA103 in Fig. 12). Deformation is thus permitted to occur everywhere in the areas of the mesh that represent central and western Honduras. The fit of model CA103 to the station velocities in eastern Honduras and at most locations in central and western Honduras is remarkably good (Fig 13), with an overall reduction of ∼40 per cent in the least-squares fit relative to that for model CA102 (Fig. 12). Its primary shortcoming is its poor fit to the westward motions of GPS stations around the Gulf of Fonseca and in zone 2a of southern Honduras.

Model CA104 simulates the driving condition that Alvarez-Gomez *et al.* (2008) impose on their FEM, in which Caribbean Plate motion is imposed only at the nodes that define the eastern edge of the block that represents the Caribbean Plate (shown by inset CA104 in Fig. 12). Model CA104 does not significantly
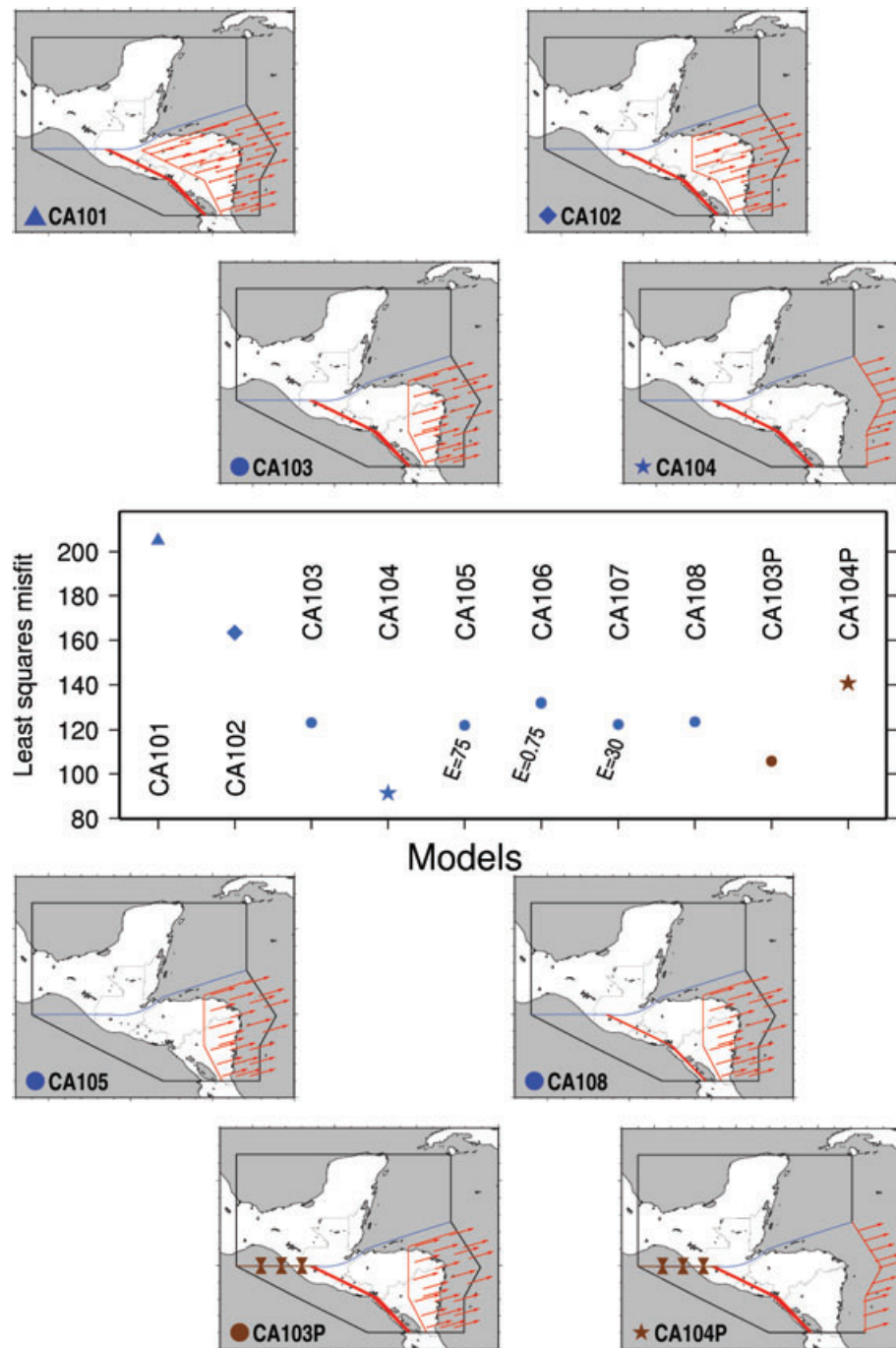
**Figure 12.** Finite element models described in the text and Table 2 and their least-squares misfits ($\chi^2$) to the GPS velocities discussed in the text. Blue lines indicate faults along which a constraint of strike-slip motion is imposed. Brown symbols show faults that are pinned and hence not permitted to slip. Each red arrow shows the Caribbean–North America Plate movement that is prescribed for a node at either the base of the FEM or along its edge nodes (models CA104 and CA104P). Numbers in the middle panel are the Young's modulus values used for the weak volcanic zone (GPa). Models for which Young's modulus is not specified employ a value of 7.5 GPa.

improve the fit to the GPS velocities in western Honduras (Fig. 13), but fits the measured velocities in southern Honduras better than does model CA103. All of the improvement in the least-squares fit for model CA104 is attributable to its superior fit to the velocities for sites in southern Honduras. Although CA104 fits the data better than any other model we tested, it predicts that sites in eastern Honduras move several mm yr$^{-1}$ to the west, in disagreement with the station velocities measured at all four sites in eastern Honduras

(Fig. 4). It thus fails to match the observed velocity pattern, despite its modestly improved fit to the station velocities in southern Honduras.

None of the models that adopt different assumed strengths for the Central American volcanic arc (CA105–CA108) significantly improve the fit relative to model CA103 (Fig. 12). Interestingly, model CA105, in which the weak zone is discarded altogether, fits the data better than any of the models that incorporate a weak zone (CA103
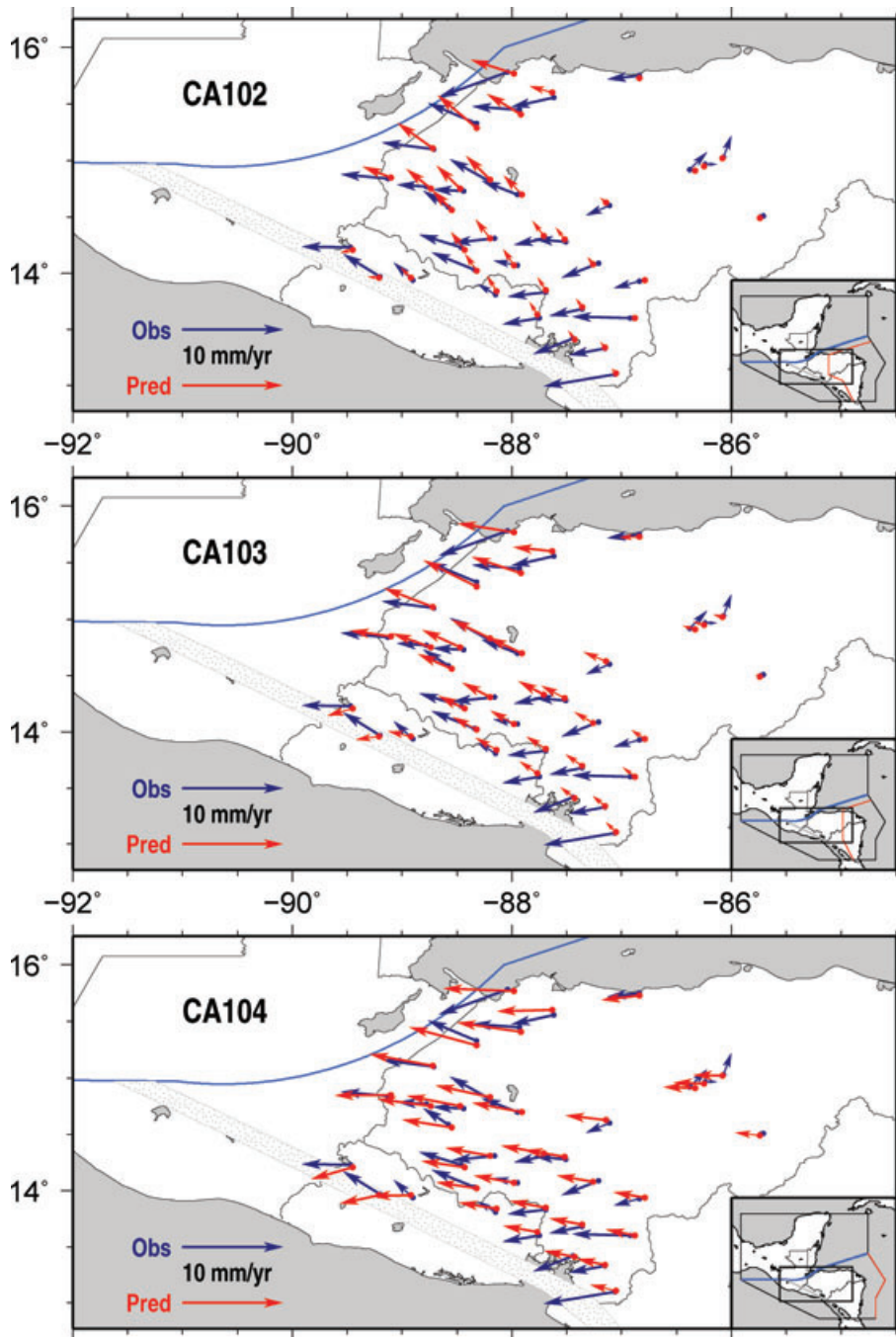
**Figure 13.** Comparison of observed GPS velocities (blue) to velocities predicted (red) by models CA102, CA103 and 104. All velocities are relative to the Caribbean Plate. Insets show FEM geometries. Red lines in the insets indicate the geographic limits of the basal or edge nodes that are used to drive each model (also shown in Fig. 12). In models CA102, CA103 and CA104, the nodes used to drive deformation of the mesh are moved progressively farther east of the study area. All other elements of these three models are the same.

and CA106–CA108). By implication, the GPS velocities from Honduras and El Salvador contain little or no useful information about the strength of the volcanic zone. This corroborates modelling results described in the previous section, in which the influence of the weak volcanic zone in an idealized FEM does not extend significantly beyond the region where the volcanic arc intersects the main plate boundary faults (Figs 10b and c).

Model CA103P, in which the Caribbean–North America Plate boundary west of the volcanic arc is pinned in order to force distributed deformation to accommodate the plate motion, predicts more rapid rates of westward motion (by ∼1–2 mm yr$^{-1}$ at most locations) than does model CA103 (Fig. 14). Its fit to the velocity field is modestly (10 per cent) better than that of model CA103 (Fig. 12), with most residual motions slower than ∼2 mm yr$^{-1}$ (Fig. 14). Model CA103P fits the well-determined velocity at continuous GPS station GUAT (located at the western limit of the velocity field in Fig. 14) better than model CA103. Neither of the two models successfully fits the GPS station velocities from southern Honduras, where the residual station motions for both models point systematically toward the Gulf of Fonseca (left-hand column
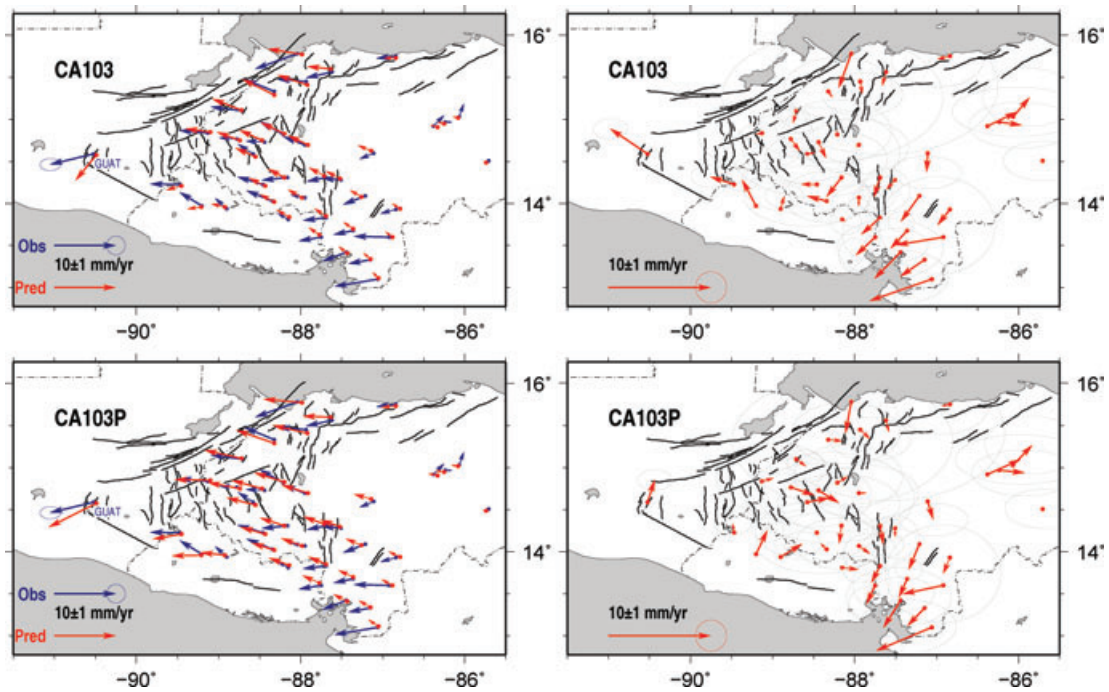
**Figure 14.** Left-hand column: comparison of observed (blue) and predicted (red) GPS velocities for models CA103 and CA103P. All velocities are relative to the Caribbean Plate. Models CA103 and CA103P differ only in that a pinned-fault constraint is imposed in the latter model along the plate boundary west of the volcanic arc (see Fig. 12). Right-hand column: residual velocities for models CA103 and 103P, defined as the predicted velocities subtracted from the observed velocities. The grey ellipses are the 2-D, 1-$\sigma$ velocity uncertainties.

of Fig. 14). The merits and shortcomings of both of these models are discussed further in Section 7.2.

Model CA104P also employs a pinned plate boundary west of the volcanic arc, but is driven by nodes at the eastern edge of the mesh, similar to model CA104. It fits the GPS velocity field worse than models CA103P and CA104 (Figs 12 and 15). In particular, it predicts station motions that are systematically faster than the observed rates at nearly all locations (Fig. 15) and also misfits the directions at most sites. Like model CA104, model CA104P predicts that stations in eastern Honduras move to the west at rates of 2–4 mm yr$^{-1}$, in conflict with the available geological and geodetic evidence (DeMets *et al.* 2007; Rogers & Mann 2007).

*6.2.3 Fits of straight-fault models CA203 and CA203P*

Model CA203, which employs a straight trace for the Motagua fault, fits the station velocities worse than model CA103, which employs a curved fault trace (Fig. 16). The model predicts that almost no deformation occurs in northern Central America (Fig. 16), in marked contrast with the predictions of the other models described above. The comparison indicates that the curved trace of the Motagua fault significantly influences the predicted deformation, primarily by impeding eastward motion of the western end of the Caribbean Plate (i.e. southern Guatemala and western Honduras) due to the oblique orientation of the fault west of 90°W relative to the east–northeast direction of the Caribbean Plate relative to North America west of 90°W.

Model CA203P, which incorporates a straight trace for the Motagua fault and pins the plate boundary west of the volcanic arc (Fig. 16), correctly predicts that west-directed deformation occurs in much of the study area, but predicts deformation rates that are consistently slower than the measured rates. Neither of the straight-fault

models therefore fits the GPS velocities as well as their curved-fault counterparts CA103 and CA103P. We conclude that the orientation and curved trace of the Motagua fault play an important role in the regional deformation.

# 7 DISCUSSION AND CONCLUSIONS

## 7.1 Observations

Our new GPS measurements reveal for the first time the first-order features of present deformation in Honduras and show that the Honduran velocity field is dominated by several mm yr$^{-1}$ of westward motion relative to locations in eastern Honduras and the Caribbean Plate interior (Fig. 7). The cumulative stretching across the Honduran rifts with respect to sites in the Caribbean Plate interior is 4–5 mm yr$^{-1}$ (Fig. 4). More rapid westward motions of $7.3 \pm 1.1$ and 11–12 mm yr$^{-1}$ are measured at station GUAT within the Guatemala City graben and two sites west of the Guatemala City graben (Lyon-Caen *et al.* 2006), indicating that extension occurs nearly everywhere south of the Motagua fault.

The data indicate that active extension across the broad deforming zone in Honduras and Guatemala siphons off more than half of the 19–20 mm yr$^{-1}$ of plate boundary slip that is carried by the Motagua and Polochic faults in eastern Guatemala. By implication, less than 10 mm yr$^{-1}$ of motion is carried west to the Middle America trench by faults or other structures that are located west or north of the Motagua fault (e.g. the Polochic fault or structures in southern Mexico).

## 7.2 Preferred models

Three FEMs, CA103, CA103P and CA104, fit the GPS velocities well. Model CA104 gives the best least-squares fit, but incorrectly
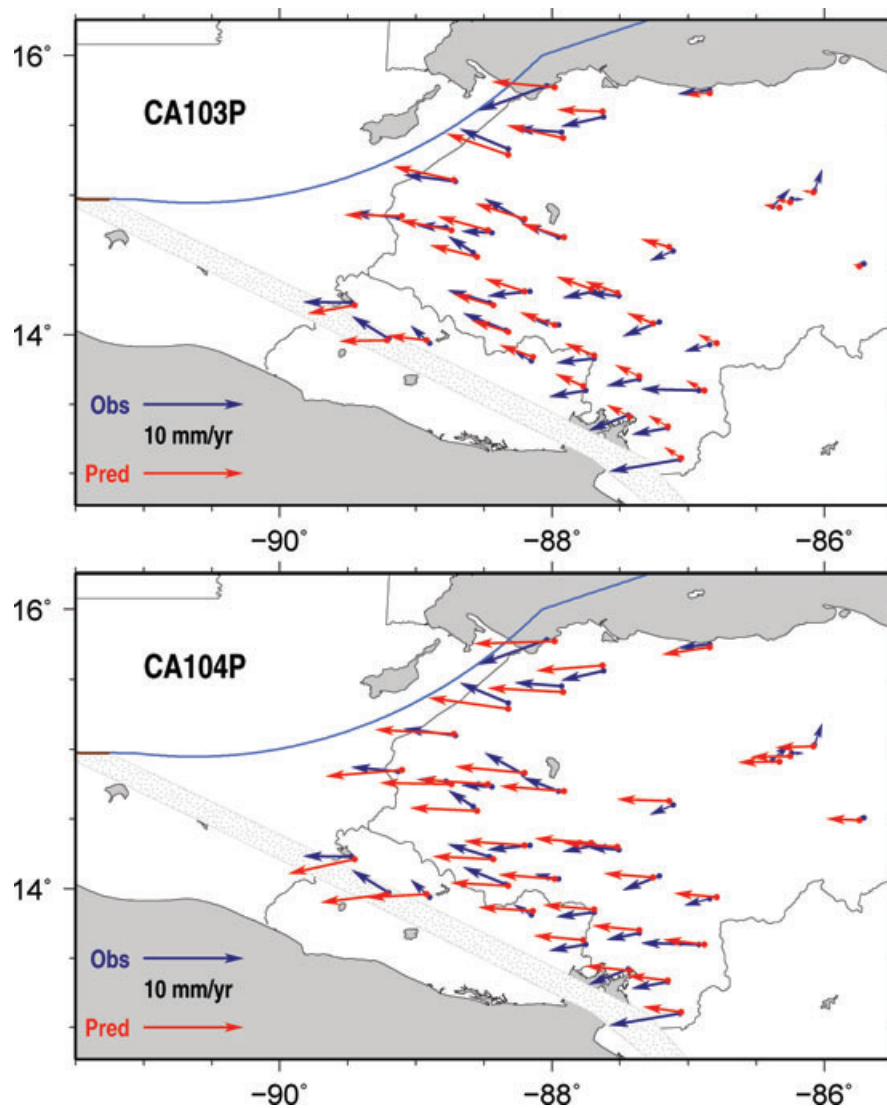
**Figure 15.** Comparison of observed (blue) and predicted (red) GPS velocities for models CA103P and CA104P. All velocities are relative to the Caribbean Plate. Both models are driven by the edge nodes along the eastern limit of the FEM (also see Fig. 12). The plate boundary fault west of the volcanic arc is free to move in CA103, but pinned in CA103P.

predicts that significant stretching occurs in central Honduras, where none is observed. In contrast, models CA103 and CA103P, which are driven by basal drag beneath eastern Honduras and areas farther east, predict little or no deformation in eastern Honduras, in accord with the GPS velocities and geological evidence described by Rogers *et al.* (2002). The velocities predicted by models CA103 and CA103P also agree well with GPS velocities measured elsewhere in Honduras, with the exception of stations around the Gulf of Fonseca, where none of the models fit the measured velocities (Fig. 14).

Models CA103 and CA103P differ primarily in the deformation that each predicts in southern Guatemala (Fig. 17). At the continuous GPS station GUAT, model CA103P predicts motion that agrees well with the measured station velocity. In contrast, model CA103 predicts motion that is only half as fast and significantly anticlockwise from the measured motion (Fig. 14). Model CA103P also predicts motions that agree better with velocities measured at nearby sites in western El Salvador.

Models CA103 and CA103P both predict principal strains that successfully match the deformation pattern implied by earthquakes

in Honduras (Fig. 17). Both models predict that the principal strains in much of Honduras are extensional (Fig. 17) and that the principal strain-rate axes rotate clockwise from E–W in northern and central Honduras to NW in western Honduras. These predictions agree remarkably well with the maximum horizontal stresses of normal-faulting earthquakes in Honduras, which rotate progressively clockwise from an E–W orientation in zone 4 of northern Honduras (Fig. 17) to WNW and then NW orientations in zones 2a and 1 of central and western Honduras.

The principal strains predicted by models CA103 and CA103P differ significantly in southern Guatemala (Fig. 17). Model CA103P predicts that the principal strain in southern Guatemala is extensional and oriented east–west, and that strain rates increase in magnitude from western Honduras to southern Guatemala. In contrast, model CA103 predicts low strain rates in both southern Guatemala and western Honduras. For comparison, the level of earthquake activity in the Guatemala City and Ipala grabens of southern Guatemala exceeds that of the Honduran grabens farther east (Plafker 1976; Langer & Bollinger 1979, Fig. 3), consistent with more rapid strain accumulation and release in southern Guatemala
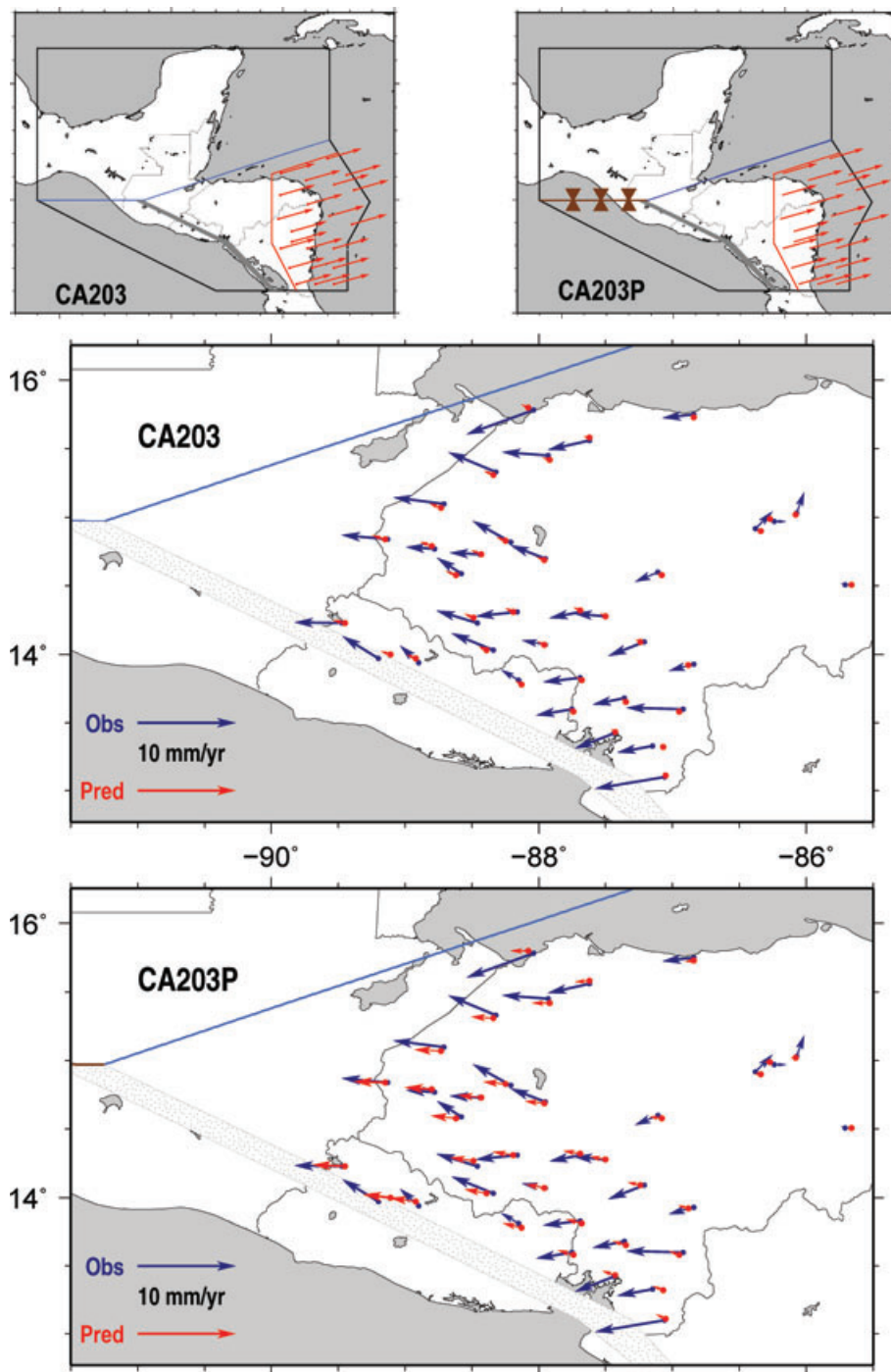
**Figure 16.** Test of FEMS with straight plate boundary faults instead of a curved Motagua fault in Central America. Please see text for further discussion. Insets shown at the top specify the model driving conditions and kinematic constraints. The symbols and other features shown in the insets are defined in the caption to Fig. 12.

than western Honduras. In addition, normal-faulting earthquakes with east–west tensional axes occur in both the Ipala and Guatemala City grabens (Fig. 17; Langer & Bollinger 1979; Guzman-Speziale 2001), consistent with the direction of extension that is predicted by model CA103P, but not by model CA103.

In southern Mexico, model CA103P predicts that the principal strains at locations northwest from the plate boundary faults consist of northeast–southwest shortening (Fig. 17). This agrees with geological evidence for northeast–southwest directed reverse faulting

in this region (Guzman-Speziale & Meneses-Rocha 2000) and with the compressional axis for a single thrust-faulting earthquake in Chiapas (Fig. 17).

### 7.3 Modelling synthesis and comparison to prior results

We conclude that a FEM that incorporates the curved trace of the Motagua fault and is driven by Caribbean–North America Plate motion via basal drag as far west as eastern Honduras successfully
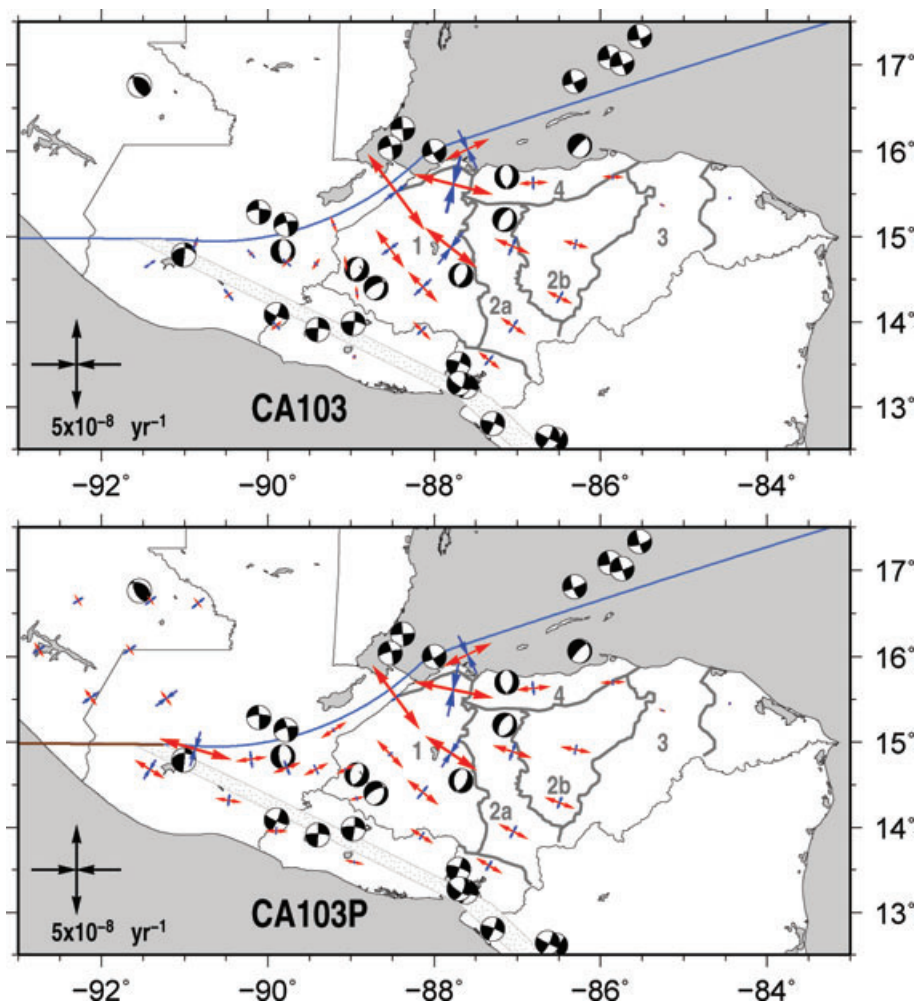
**Figure 17.** Principal strain-rate axes and magnitudes predicted by models CA103 and CA103P. Red and blue arrows specify extensional and compressional strain rates, respectively. The earthquake focal mechanisms are from the Harvard centroid moment-tensor database for the period 1976–2008. Bold lines indicate the limits of morphotectonic zones shown in the previous figures and described in the text.

captures many important aspects of present deformation in northern Central America. Substituting the curved fault trace with a straight trace that is parallel to the Swan Islands fault results in a FEM that predicts either no deformation (CA203 in Fig. 16) or too little deformation (CA203P in Fig. 16), thereby demonstrating that the plate boundary geometry significantly influences the regional deformation pattern. A simple consideration of the plate motion direction relative to the azimuth of the Motagua fault helps explain why extension occurs throughout so much of Honduras and southern Guatemala. West of 90°W, the azimuth of the Motagua fault varies between N85°W and N90°W, whereas the Caribbean–North America Plate direction predicted at locations west of 90°W is N73°E ± 1.5°. The fault therefore strikes 17–22° clockwise from the plate slip direction and impedes the eastward movement of lithosphere south of the fault in southern Guatemala. The extension in southern Guatemala and western Honduras, at the trailing western edge of the Caribbean Plate, thus appears to result from partial pinning of the western wedge of the Caribbean Plate due to the obliquely convergent angle between the western end of the Motagua fault and the direction of Caribbean–North America Plate motion. In this regard, our results confirm conclusions previously reached by Alvarez-Gomez *et al.* (2008) regarding the primary cause of extension south of the Motagua fault.

The curvature of the Motagua fault also influences the regional deformation (Fig. 17). The Caribbean–North America Plate direction varies by less than 0.5° in northern Central America. The angle between the irregular trace of the fault and the plate motion direction therefore changes along strike, giving rise to changes in the orientation of the principal strain-rate axes along the fault (Fig. 17). Rogers & Mann (2007) attribute along-strike variations in the predominant structures in the borderlands of the Motagua and Swan Islands faults to the changing angle between the azimuths of these faults and the local direction of plate motion. Our results corroborate their conclusion.

### 7.4 Outstanding questions and future work

The results described above leave unanswered many questions about the regional tectonics. For example, is extension evenly distributed across the Honduran grabens or focused within just a few grabens? Does the extension in southern Honduras also extend to adjacent parts of Nicaragua? How might the elastic effects from locked faults in the study area influence the modelling and interpretation of the velocity field, particularly in areas such as southern Guatemala where most sites may be close enough to active faults to experience their elastic effects? How might variations in the elastic thickness of the

crust influence the fit? Is the regional deformation significantly influenced by other forces such as possible mantle upwelling beneath Honduras (Rogers *et al.* 2002) or roll-back of the Middle America trench inferred by Phipps Morgan *et al.* (2008)?

Efforts to better understand the complex tectonics of northern Central America would benefit substantially from new GPS sites in critical areas such as southern Guatemala and southern Mexico. Additional measurements at existing sites are also needed to reduce the substantial uncertainties in the present velocity field. Velocity fields derived from all of the regional GPS data using identical data processing procedures and reference frames are also needed to minimize subtle artefacts that can otherwise affect velocity fields via reference frame biases and different processing procedures. Finally, additional GPS sites are needed in the interiors of Nicaragua and Honduras to better define the geographic limits of the stable parts of the plate interior and identify a suitable set of basal driving conditions for modelling the regional deformation.

## REFERENCES

Altamimi, Z., Collilieux, X., Legrand, J., Garayt, B. & Boucher, C., 2007. ITRF2005: a new release of the International Terrestrial Reference Frame based on time series of station positions and Earth orientation parameters, *J. geophys. Res.,* **112,** B09401, doi:10.10292007JB004949.

Alvarado, D., 2008. Crustal deformation of the Salvadoran-Nicaraguan forearc at the Gulf of Fonseca: a multidisciplinary tectonic study, M.S. thesis, University of Wisconsin-Madison, Madison.

Alvarez-Gomez, J.A., Meijer, P.T., Martinez-Diaz, J.J. & Capote, R., 2008. Constraints from finite element modeling on the active tectonics of northern Central America and the Middle America Trench, *Tectonics,* **27,** TC1008, doi:10.1029/2007TC002162.

Blewitt, G., 2008. Fixed point theorems of GPS carrier phase ambiguity resolution and their application to massive network processing: Ambizap, *J. geophys. Res.,* **113,** B12410, doi:10.1029/2008JB005736.

Burkart, B., 1978. Offset across the Polochic fault of Guatemala and Chiapas, Mexico, *Geology,* **6,** 328–332.

Burkart, B., 1983. Neogene North American-Caribbean plate boundary: offset along the Polochic fault, *Tectonophysics,* **99,** 251–270.

Burkart, B. & Self, S., 1985. Extension and rotation of crustal blocks in northern Central America and effect on the volcanic arc, *Geology,* **13,** 22–26.

Burkart, B., Deaton, B.C., Dengo, C. & Moreno, G., 1987. Tectonic wedges and offset Laramide structures along the Polochic fault of Guatemala and Chiapas, Mexico: reaffirmation of large Neogene displacement, *Tectonics,* **6,** 411–422.

Caceres, D., Monterroso, D. & Tavakoli, B., 2005. Crustal deformation in northern Central America, *Tectonophysics,* **404,** 119–131.

Correa-Mora, F. *et al.*, 2009. Evidence for weak coupling of the Cocos plate subduction interface and strong coupling of the volcanic arc faults from modeling of GPS data: EL Salvador and Nicaragua, *Geophys. J. Int.,* submitted.

Corti, G., Carminati, E., Mazzarini, F. & Garcia, M.O., 2005. Active strike-slip faulting in El Salvador, Central America, *Geology,* **33,** 989–992.

Cox, R.T., Lumsden, D.N., Gough, K., Lloyd, R. & Talnagi, J., 2008. Investigation of late Quaternary fault block uplift along the Motagua/Swan Islands fault system: implications for seismic/tsunami hazard for the Bay of Honduras, *Tectonphysics,* **457,** 30–41.

DeMets, C., 2001. A new estimate for present-day Cocos-Caribbean plate motion: implications for slip along the Central American volcanic arc, *Geophys. Res. Lett.,* **28,** 4043–4046.

DeMets, C., Mattioli, G., Jansma, P., Rogers, R., Tenorio, C. & Turner, H.L., 2007. Present motion and deformation of the Caribbean plate: constraints from new GPS geodetic measurements from Honduras and Nicaragua, in *Geologic and Tectonic Development of the Caribbean Plate in Northern Central America,* pp. 21–36, ed. Mann, P., *Geol. Soc. Am. Spec. Paper 428*, The Geological Society of America, Boulder, doi:10.1130/2007.2428(01).

Ferrari, L., Pasquare, G. & Zilioli, E., 1994. Kinematics and seismotectonics of a segment of the North-Caribbean plate boundary: a remote sensing and field study of the Jocotan fault system in Guatemala, in *Geology from Space,* Vol. 2320, pp. 55–63, ed. Zilioli, E., SPIE, Bellingham, doi:10.1117/12.197300.

Gordon, M.B. & Muehlberger, W.R., 1994. Rotation of the Chortis block causes dextral slip on the Guayape fault, *Tectonics,* **13,** 858–872.

Guzman-Speziale, M., 2001. Active seismic deformation in the grabens of northern Central America and its relationship to the relative motion of the North America-Caribbean plate boundary, *Tectonophysics,* **337,** 39–51.

Guzman-Speziale, M. & Meneses-Rocha, J.J., 2000. The North America-Caribbean plate boundary west of the Motagua-Polochic fault system: a fault jog in southeastern Mexico, *J. South Am. Earth Sci.,* **13,** 459–468.

Guzman-Speziale, M., Pennington, W.D. & Matumoto, T., 1989. The triple junction of the North America, Cocos, and Caribbean plates: seismicity and tectonics, *Tectonics,* **8,** 981–997.

Heflin, M. *et al.*, 1992. Global geodesy using GPS without fiducial sites, *Geophys. Res. Lett.,* **19,** 131–134.

Langer, C.J. & Bollinger, G.A., 1979. Secondary faulting near the terminus of a seismogenic strike-slip fault: aftershocks of the 1976 Guatemala earthquake, *Bull. seism. Soc. Am.,* **69,** 427–444.

Lyon-Caen, H. *et al.*, 2006. Kinematics of the North American-Caribbean-Cocos plates in Central America from new GPS measurements across the Polochic-Motagua fault system, *Geophys. Res. Lett.,* **33,** L19309, doi:10.1029/2006GL027694.

Malfait, B.T. & Dinkelman, M.G., 1972. Circum-Caribbean tectonic and igneous activity and the evolution of the Caribbean plate, *Geol. Soc. Am. Bull.,* **83,** 251–271.

Manton, W.I., 1987. Tectonic interpretation of the morphology of Honduras, *Tectonics,* **6,** 633–651.

Mao, A., Harrison, C.G.A. & Dixon, T.H., 1999. Noise in GPS coordinate time series, *J. geophys. Res.,* **104,** 2797–2816.

Marquez-Azua, B. & DeMets, C., 2003. Crustal velocity field of Mexico from continuous GPS measurements, 1993 to June, 2001: implications for the neotectonics of Mexico, *J. geophys. Res.,* **108**(B9), 2450, doi:10.1029/2002JB002241.

Matumoto, T. & Latham, G.V., 1976. Aftershocks of the Guatemalan earthquake of February 4, 1976, *Geophys. Res. Lett.,* **3,** 599–602.

Muehlberger, W.R. & Ritchie, A.W., 1975. Caribbean-Americas plate boundary in Guatemala and southern Mexico as seen on Skylab IV orbital photography, *Geology,* **3,** 232–235.

Osiecki, P.S., 1981. Estimated intensities and probable tectonic sources of historic (pre-1898) Honduran earthquakes, *Bull. seism. Soc. Am.,* **71,** 865–881.

Phipps Morgan, J., Ranero, C.R. & Vannucchi, P., 2008. Intra-arc extension in Central America: links between plate motions, tectonics,

volanism, and geochemistry, *Earth planet. Sci. Lett.,* **272,** 365–371, doi:10.1016/j.epsl.20087.05.004.

Plafker, G., 1976. Tectonic aspects of the Guatemala earthquake of 4 February 1976, *Science,* **193,** 1201–1208.

Rogers, R.D., 2003. Jurassic-Recent tectonic and stratigraphic history of the Chortis block of Honduras and Nicaragua (northern Central America), *PhD thesis*, University of Texas at Austin, Austin.

Rogers, R.D. & Mann, P., 2007. Transtensional deformation of the western Caribbean-North America plate boundary zone, in *Geologic and Tectonic Development of the Caribbean Plate Boundary in Northern Central America,* pp. 37–64, ed. Mann P. *Geol. Soc. Am. Spec. Paper 428*, The Geological Society of America, Boulder, doi:10.1130/2007.2428(02).

Rogers, R.D., Karason, H. & Hilst, R.D. van der, 2002. Epeirogenic uplift above a detached slab in northern Central America, *Geology,* **30,** 1031–1034.

Rosencrantz, E. & Mann, P., 1991. SeaMARC II mapping of transform faults in the Cayman Trough, Caribbean Sea, *Geology,* **19,** 690–693.

Schwartz, D.P., Cluff, L.S. & Donnelly, T.W., 1979. Quaternary faulting along the Caribbean-North American plate boundary in Central America, *Tectonophysics,* **52,** 432–445.

ten Brink, U.S., Katzman, R. & Lin, J., 1996. Three-dimensional models of deformation near strike-slip faults, *J. geophys. Res.,* **101,** 16 205–16 220.

Turner, H.L.I., LaFemina, P., Saballos, A., Mattioli, G.S., Jansma, P.E. & Dixon, T., 2007. Kinematics of the Nicaraguan forearc from GPS geodesy, *Geophys. Res. Lett.,* **34,** L02302, doi:10.1029/2006GL027586.

Wessel, P. & Smith, W.H.F., 1991. Free software helps map and display data, *EOS, Trans. Am. geophys. Un.,* **72,** 441–446.

White, R.A., 1985. The Guatemala earthquake of 1816 on the Chixoy-Polochic fault, *Bull. seism. Soc. Am.,* **75,** 455–473.

Zumberge, J.F., Heflin, M.B., Jefferson, D.C., Watkins, M.M. & Webb, F.H., 1997. Precise point positioning for the efficient and robust analysis of GPS data from large networks, *J. geophys. Res.,* **102,** 5005–5017.